Preface

The first edition of *Principles* was published in 1983, and the second edition 16 years later in 1999. At that time I thought the third edition would not be written until 2010 or later. However, the technology of fluorescence has advanced at an accelerating pace. Single-molecule detection and fluorescence-correlation spectroscopy are becoming almost routine. New classes of probes have appeared, such as the semiconductor nanoparticles, or QDots, and genetically engineered green fluorescent probes. Additionally, it is now becoming possible to control the excited states of fluorophores, rather than relying only on spontaneous emission. These developments are changing the paradigm of fluorescence, from a reliance on organic fluorophores, to the use of genetic engineering, nanotechnology, and near-field optics.

I wish to express my appreciation and special thanks to the individuals who have assisted me in the preparation of the book. These include Ignacy Gryczynski for assistance with the figures, Krystyna Gryczynski for drawing the figures, Joanna Malicka for proofreading the chapters, Kazik Nowaczyk for the cover design and color digitizing of all figures, Tim Oliver for typesetting, and the NIH for their support of my laboratory. And finally, Mary, for her endless hours of typing, correspondence and support.

Joseph R. Lakowicz

Instrumentation for Fluorescence Spectroscopy

2

The success of fluorescence experiments requires attention to experimental details and an understanding of the instrumentation. There are also many potential artifacts that can distort the data. Light can be detected with high sensitivity. As a result, the gain or amplification of instruments can usually be increased to obtain observable signals, even if the sample is nearly nonfluorescent. These signals seen at high amplification may not originate with the fluorophore of interest. Instead, the interference can be due to background fluorescence from the solvents, light leaks in the instrumentation, emission from the optical components, stray light passing through the optics, light scattered by turbid solutions, and Rayleigh and/or Raman scatter, to name a few interference sources.

An additional complication is that there is no ideal spectrofluorometer. The available instruments do not yield true excitation or emission spectra. This is because of the nonuniform spectral output of the light sources and the wavelength-dependent efficiency of the monochromators and detector tubes. The polarization or anisotropy of the emitted light can also affect the measured fluorescence intensities because the efficiency of gratings depends on polarization. It is important to understand and control these numerous factors. In this chapter we will discuss the properties of the individual components in a spectrofluorometer, and how these properties affect the observed spectral data. These instrumental factors can affect the excitation and emission spectra, as well as the measurement of fluorescence lifetimes and anisotropies. Additionally, the optical properties of the samples—such as optical density and turbidity—can also affect the spectral data. Specific examples are given to clarify these effects and the means to avoid them.

2.1. SPECTROFLUOROMETERS

2.1.1. Spectrofluorometers for Spectroscopy Research

With most spectrofluorometers it is possible to record both excitation and emission spectra. An emission spectrum is the wavelength distribution of an emission measured at a single constant excitation wavelength. Conversely, an excitation spectrum is the dependence of emission intensity, measured at a single emission wavelength, upon scanning the excitation wavelength. Such spectra can be presented on either a wavelength scale or a wavenumber scale. Light of a given energy can be described in terms of its wavelength λ, frequency ν, or wavenumber. The usual units for wavelength are nanometers, and wavenumbers are given in units of cm^{-1}. Wavelengths and wavenumbers are easily interconverted by taking the reciprocal of each value. For example, 400 nm corresponds to $(400 \times 10^{-7}\ cm)^{-1} = 25{,}000\ cm^{-1}$. The presentation of fluorescence spectra on the wavelength or wavenumber scale has been a subject of debate. Admittedly, the wavenumber scale is linear in energy. However, most commercially available instrumentation yields spectra on the wavelength scale, and such spectra are more familiar and thus easier to interpret visually. Since corrected spectra are not needed on a routine basis, and since accurately corrected spectra are difficult to obtain, we prefer to use the directly recorded technical or uncorrected spectra on the wavelength scale.

For an ideal instrument, the directly recorded emission spectra would represent the photon emission rate or power emitted at each wavelength, over a wavelength interval determined by the slit widths and dispersion of the emission
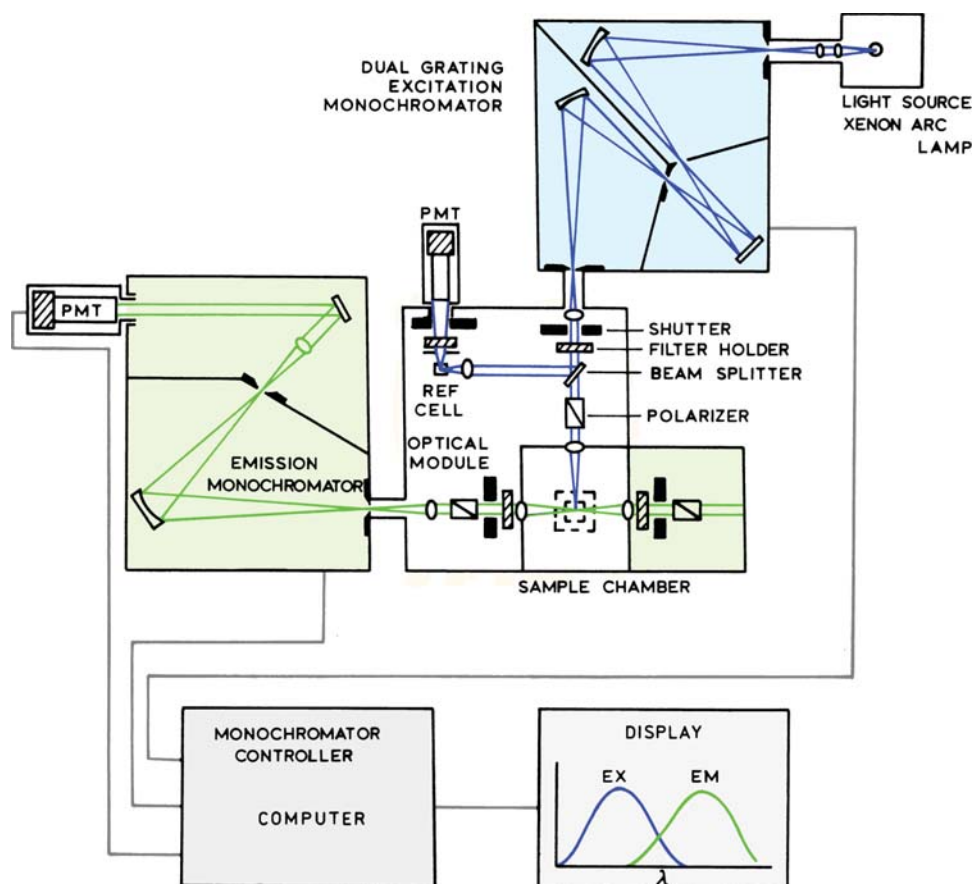
Figure 2.1. Schematic diagram of a spectrofluorometer [1].

monochromator. Similarly, the excitation spectrum would represent the relative emission of the fluorophore at each excitation wavelength. For most fluorophores the quantum yields and emission spectra are independent of excitation wavelength. As a result, the excitation spectrum of a fluorophore can be superimposable on its absorption spectrum. However, such identical absorption and excitation spectra are rarely observed because the excitation intensity is different at each wavelength. Even under ideal circumstances such correspondence of the excitation and absorption spectra requires the presence of only a single type of fluorophore, and the absence of other complicating factors, such as a nonlinear response resulting from a high optical density of the sample or the presence of other chromophores in the sample. Emission spectra recorded on different instruments can be different because of the wavelength-dependent sensitivities of the instruments.

Figure 2.1 shows a schematic diagram of a general-purpose spectrofluorometer: this instrument has a xenon lamp as a source of exciting light. Such lamps are generally useful because of their high intensity at all wavelengths ranging upward from 250 nm. The instrument shown is equipped with monochromators to select both the excitation and emission wavelengths. The excitation monochromator in this schematic contains two gratings, which decreases stray light, that is, light with wavelengths different from the chosen one. In addition, these monochromators use concave gratings, produced by holographic means to further decrease stray light. In subsequent sections of this chapter we will discuss light sources, detectors and the importance of spectral purity to minimize interference due to stray light. Both monochromators are motorized to allow automatic scanning of wavelength. The fluorescence is detected with photomultiplier tubes and quantified with the appropriate electronic devices. The output is usually presented in graphical form and stored digitally.

The instrument schematic also shows the components of the optical module that surrounds the sample holder. Ver-

satile and stable optical components are indispensable for a research spectrofluorometer. The module shown in Figure 2.1 contains a number of convenient features that are useful on a research instrument. Shutters are provided to eliminate the exciting light or to close off the emission channel. A beam splitter is provided in the excitation light path. This splitter reflects part of the excitation light to a reference cell, which generally contains a stable reference fluorophore. The beam splitter consists of a thin piece of clear quartz, which reflects about 4% of the incident light. This amount is generally adequate for a reference channel that frequently contains a highly fluorescent quantum counter (Section 2.8.1). The intensity from the standard solution is typically isolated with a bandpass filter, and is proportional to the intensity of the exciting light. Changes in the intensity of the arc lamp may be corrected for by division of the intensity from the sample by that of the reference fluorophore.

Polarizers are present in both the excitation and emission light paths. Generally, the polarizers are removable so that they can be inserted only for measurements of fluorescence anisotropy, or when it is necessary to select for particular polarized components of the emission and/or excitation. Accurate measurement of fluorescence anisotropies requires accurate angular positioning of the polarizers. The polarizer mounts must be accurately indexed to determine the angular orientation. The optical module shown in Figure 2.1 has an additional optical path on the right side of the sample holder. This path allows measurement of fluorescence anisotropy by the T-format method (Chapter 10). There are many occasions where the additional light path is necessary or convenient for experiments, but with modern electronics it is usually not necessary to use the T-format for anisotropy measurements.

The present trend is toward small compact spectrofluorometers, with all the optical components in a single enclosure. Such instruments are easy to maintain because there is little opportunity to alter the configuration. A modular instrument has some advantages in a spectroscopy laboratory. For instance, if the xenon lamp and monochromator are removable, a laser source can be used in place of the arc lamp. On some occasions it is desirable to bypass the emission monochromator and use bandpass filters to collect as much of the emission as possible. Such experiments are possible if the emission monochromator is removable. If the monochromator cannot be removed the gratings can act like mirrors if set at the zero-order diffraction or a wavelength of zero. If the wavelength is set to zero the monochromator

typically transmits all wavelengths. Filters can be used to isolate the desired range of wavelengths.

It is convenient if the instrument has a versatile sample holder. If the research involves anisotropy measurements it will often be necessary to measure the fundamental anisotropy (r_0) in the absence of rotational diffusion. This is accomplished at low temperature, typically –50°C in glycerol. Low temperature can only be achieved if the sample holder is adequately sized for a high rate of coolant flow, has good thermal contact with the cuvette, and is insulated from the rest of the instrument. Many cuvette holders can maintain a temperature near room temperature, but may not be able to maintain a temperature much above or below that.

Another useful feature is the ability to place optical filters into the excitation or emission light path. Filters are often needed, in addition to monochromators, to remove unwanted wavelengths in the excitation beam, or to remove scattered light from the emission channel.

2.1.2. Spectrofluorometers for High Throughput

At present the design of fluorescence experiments is changing toward a multi-sample approach. Instead of detailed experiments on a single sample, the experiments are designed to include many samples. Such experiments can include binding studies, quenching, and cell-based assays. High-throughput screening assays are used in drug discovery, often using numerous microplates, each with 384 or more wells. Such measurements are typically performed using microplate readers (Figure 2.2). The samples are contained in the wells of the microplates, which are taken inside the instrument for the measurements. Such an instrument may not provide the detailed information available using an instrument designed for spectroscopy (Figure 2.1) but can rapidly provide measurements on numerous samples.
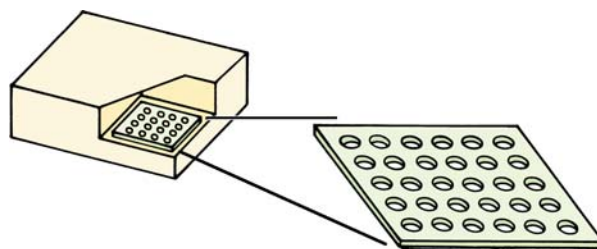

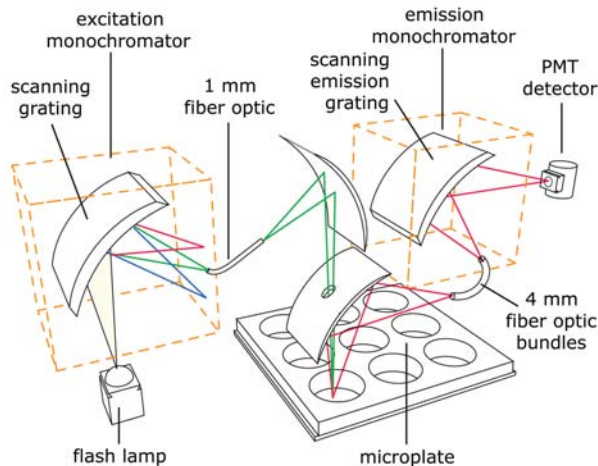Figure 2.2. Fluorescence microplate reader.

Figure 2.3. Optical path for a microplate reader [2].

Figure 2.4. Properties of the ideal components of a spectrofluorometer.

3. the monochromator efficiency must be independent of polarization; and

4. the detector (photomultiplier tube) must detect photons of all wavelengths with equal efficiency.

These characteristics for ideal optical components are illustrated in Figure 2.4. Unfortunately, light sources, monochromators, and photomultiplier tubes with such ideal characteristics are not available. As a result, one is forced to compromise on the selection of components and to correct for the nonideal response of the instrument.

An absorption spectrophotometer contains these same components, so why is it possible to record correct absorption spectra? In recording an absorption spectrum the intensity of light transmitted by the sample is measured relative to that transmitted by the blank. Comparative measurements are performed with the same components, at the same wavelengths. The nonideal behavior of the components cancels in the comparative measurements. In contrast to absorption measurements, fluorescence intensity measurements are absolute, not relative. Comparison of the sample fluorescence with a blank is not useful because the blank, in principle, displays no signal. Also, the weak background signal has an unknown spectral distribution, and thus cannot be used for correction of the wavelength dependence of the optical components. Hence, the opportunity for internal compensation is limited. As will be described below, a limited number of standard spectra are available for correction purposes. Corrected emission spectra are provided in Appendix I.

The optics used in microplate readers are different than in an instrument designed for use with a cuvette. Microwell plates must remain horizontal, and it is not possible to use right-angle observation as can be used with a cuvette. Figure 2.3 shows a typical optical path for microplate readers. The light source is a xenon flash lamp, which is becoming more common in fluorescence instruments. The desired excitation wavelength is selected using a monochromator. A unique feature is the mirror with a hole to transmit the excitation. The fluorescence, which occurs in all directions, is directed toward the detector optics by the same mirror. Typically, the microplate is moved to position each well in the observation path by an *x–y* scanning stage. Some microplate readers include a second mirror under the microplate to facilitate cell-based assays or absorption measurements. Microplate readers are typically used for intensity measurements on a large number of samples. Microplate readers have become available for research spectrofluorometers allowing collection of spectra, anisotropies, and lifetimes.

2.1.3. An Ideal Spectrofluorometer

In an ideal case the recorded excitation and emission spectra would represent the relative photon intensity per wavelength interval. To obtain such "corrected" emission spectra the individual components must have the following characteristics:

1. the light source must yield a constant photon output at all wavelengths;

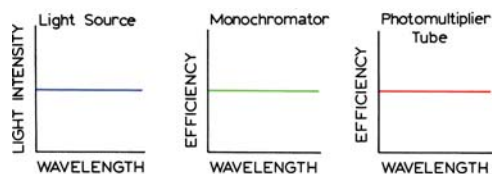2. the monochromator must pass photons of all wavelengths with equal efficiency;

2.1.4. Distortions in Excitation and Emission Spectra

To record an excitation spectrum, the emission monochromator is set at the desired wavelength, generally the emission maximum. The excitation monochromator is then scanned through the absorption bands of the fluorophore. The observed signal is distorted for several reasons:

1. The light intensity from the excitation source is a function of wavelength. Even if the intensity of the exciting light is monitored via the beam splitter shown in Figure 2.1, and corrected by division, the response of the reference solution or detector may be dependent upon wavelength.
2. The transmission efficiency of the excitation monochromators is a function of wavelength.
3. The optical density of the sample may exceed the linear range, which is about 0.1 absorbance units, depending upon sample geometry.

Emission spectra are recorded by choosing an appropriate excitation wavelength and scanning wavelength with the emission monochromator. In addition to the factors discussed above, the emission spectrum is further distorted by the wavelength-dependent efficiency of the emission monochromator and photomultiplier. The emission spectrum can also be distorted by absorption of the sample.

2.2. LIGHT SOURCES

We now describe the individual components of a spectrofluorometer. The general characteristics of these components are considered along with the reason for choosing specific components. Understanding the characteristics of these components allows one to understand the capabilities and limitations of spectrofluorometers. We will first consider light sources.

2.2.1. Arc and Incandescent Xenon Lamps

At present the most versatile light source for a steady-state spectrofluorometer is a high-pressure xenon (Xe) arc lamp. These lamps provide a relatively continuous light output from 250 to 700 nm (Figure 2.5), with a number of sharp lines occurring near 450 nm and above 800 nm. Xenon arc lamps emit a continuum of light as a result of recombination of electrons with ionized Xe atoms. These ions are generated by collisions of Xe atoms with the electrons that flow across the arc. Complete separation of the electrons from the atoms yields the continuous emission. Xe atoms that are in excited states but not ionized yield lines rather than broad emission bands. The peaks near 450 nm are due to these excited states. The output intensity drops rapidly below 280 nm. Furthermore, many Xe lamps are classified as being ozone-free, meaning that their operation does not generate
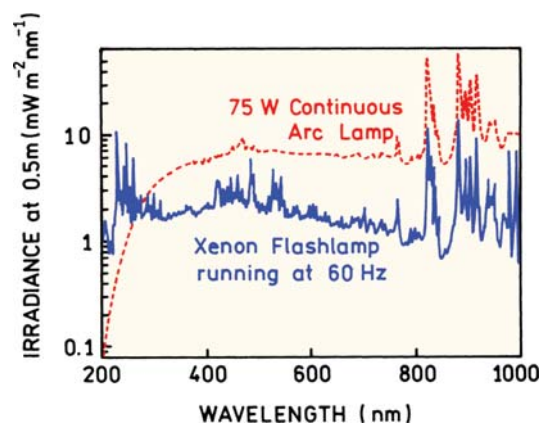

Figure 2.5. Spectral output of a continuous xenon arc lamp and a xenon flash lamp. Revised from [3]. Courtesy of Newport Corp.

ozone in the surrounding air. The quartz envelope used in such ozone-free lamps does not transmit light with wavelengths shorter than 250 nm, and the output of such lamps decreases rapidly with decreasing wavelength.

The wavelength-dependent output of Xe lamps is a major reason for distortion of the excitation spectra of compounds that absorb in the visible and ultraviolet. To illustrate this effect Figure 2.6 shows corrected and uncorrected excitation fluorescein spectra. The uncorrected spectra are recorded emission intensities with no correction for wavelength-dependent excitation intensity. The uncorrected excitation spectrum displays a number of peaks near 450 nm. These peaks are due to the output of the Xe lamp, which also displays peaks near 450 nm (Figure 2.5). Also shown in Figure 2.6 is the excitation spectrum, corrected for the wavelength-dependent output of the Xe arc lamp. A
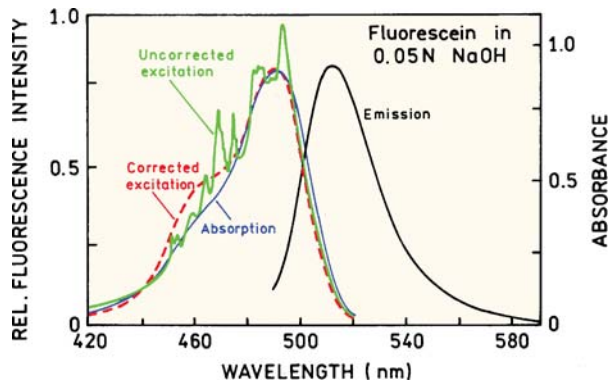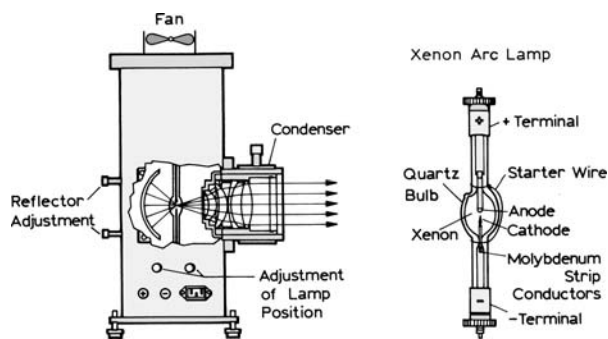

Figure 2.6. Corrected and uncorrected excitation spectra of fluorescein. From [4].

Figure 2.7. Xenon air lamp and a typical lamp housing. Revised from [5]. Courtesy of Newport Corp.

quantum counter was used in the reference channel to provide a signal proportional to the lamp intensity, and the intensity of the sample was divided by this reference intensity (Section 2.8.1). The peaks are no longer apparent in the corrected excitation spectrum, and this spectrum corresponds more closely with the absorption spectrum of fluorescein. The marked difference between the corrected and uncorrected spectra illustrates how the spectral output of the lamp influences the shape of the excitation spectra.

Xenon lamps are usually contained within specially designed housings. The arc lamp housing serves several important functions (Figure 2.7). The gas in xenon lamps is under high pressure (about 10 atmospheres), and explosion is always a danger. The housing protects the user from the lamp and also from its intense optical output. The housing also directs air over the lamp and removes excess heat and ozone. A xenon lamp that is on should never be observed directly. The extreme brightness will damage the retina, and the ultraviolet light can damage the cornea.

Another important role of the housing is for collecting and collimating lamp output, which is then focused into the entrance slit of the monochromator. Some lamp houses have mirrors behind the lamp to direct additional energy toward the output. Most of the light output originates from the small central region between the electrodes, and this spot needs to be focused on the optical entrance slit of the excitation monochromator.

Because of the heat and high intensity of a running xenon lamp, it is not practical to adjust the position of an uncovered lamp. Hence the lamp housing should have external provisions for position adjustment and focusing. The useful life of a xenon lamp is about 2000 hours. Safety glasses should be worn when handling these lamps. The

quartz envelope should not be touched, and if touched should be cleaned with a solvent such as ethanol. The fingerprint residues will char, resulting in hot spots on the quartz envelope and possible lamp failure. To protect the next person handling the disposed lamp, one should wrap the lamp in heavy paper and break the quartz envelope. It is important to pay close attention to mounting lamps in the proper orientation, which can be different for different types of lamps.
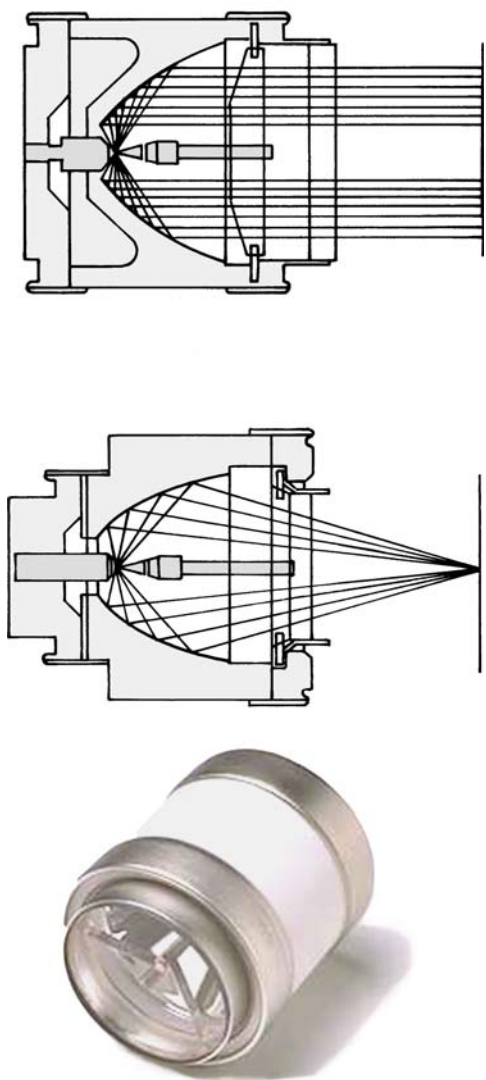
The power supplies of arc lamps are extremely dangerous, generating 25 amps at 20 volts, for a typical 450-watt lamp. Starting the lamps requires high-voltage pulses of 20 to 40 kV. This voltage can penetrate the skin, and the following high current could be lethal. Starting of xenon lamps can damage nearby sensitive electronics. The high-voltage starting pulse can destroy sensitive amplifiers or confuse computers. If possible, it is preferable to start a lamp first, and then turn on other electronic devices.

Xenon arc lamps have become more compact (Figure 2.8). These lamps typically have the arc within a parabolic reflector, which collects a large solid angle and provides a collimated output.[6] In addition to improved light collection efficiency, these lamps are compact, and as a result are found in commercial spectrofluorometers.

When using a xenon arc lamp it is important to remember the lamps emit a large amount of infrared radiation, extending beyond the wavelength range of Figure 2.5. Because of the infrared output, the lamp output cannot be passed directly through most optical filters. The filter will heat and/or crack, and the samples will be heated. When passed through a monochromator the optical components and housing serve as a heat sink. If the xenon lamp output is to be used directly, one should use a heat filter made of heat-resistant glass, which absorbs the infrared.

2.2.2. Pulsed Xenon Lamps

At present compact fluorometers and plate readers often use xenon flash lamps. The output of a xenon flash lamp is more structured than a continuous lamp (Figure 2.5). The output of a flash lamp is higher in the UV. The output intensities in Figure 2.5 are the time-averaged output of the lamp. The peak intensity of the pulses is usually higher than that of the continuous arcs. The flash lamps consume less power and generate less heat. In some cases the lack of continuous excitation can minimize photodamage to the sample.
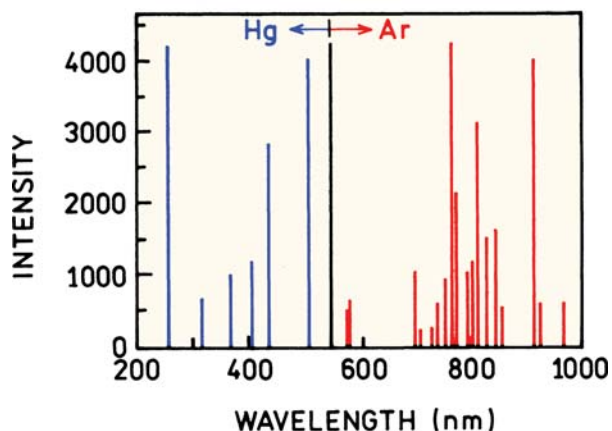
Figure 2.9. Spectral output of a low pressure mercury–argon lamp. Revised from [7]. Courtesy of Ocean Optics Inc.

Figure 2.8. Compact xenon arc lamps. Reprinted from Cermax lamp engineering guide.

2.2.3. High-Pressure Mercury (Hg) Lamps

In general Hg lamps have higher intensities than Xe lamps, but the intensity is concentrated in lines. It is usually better to choose the excitation wavelengths to suit the fluorophore, rather than vice versa. These lamps are only useful if the Hg lines are at suitable wavelengths for excitation.

2.2.4. Xe–Hg Arc Lamps

High-pressure mercury–xenon lamps are also available. These have higher intensities in the ultraviolet than Xe lamps, and the presence of Xe tends to broaden the spectral output. The output of these lamps is dominated by the Hg lines. The Hg–Xe lamp has slightly more output between the Hg lines. When first started the Hg–Xe lamp output is due mostly to Xe. As the lamp reaches operating temperature all the Hg becomes vaporized, and the Hg output increases.

2.2.5. Quartz–Tungsten Halogen (QTH) Lamps

These lamps provide continuous output in the visible and IR regions of the spectrum. Previously such lamps were not useful for fluorescence because they have low output below 400 nm, and are thus not useful for excitation of UV absorbing fluorophores. However, there is presently increasing interest in fluorophores absorbing in the red and near infrared (NIR), where the output of a QTH lamp is significant.

2.2.6. Low-Pressure Hg and Hg–Ar Lamps

These lamps yield very sharp line spectra that are useful primarily for calibration purposes (Figure 2.9). Previously the lamps contained only mercury. Some lamps now contain both mercury and argon. The mercury lines are below 600 nm and the argon lines are above 600 nm (Table 2.1). The use of these lamps for wavelength calibration is described in Section 2.3.5.

2.2.7. LED Light Sources

LEDs are just beginning to be used as light sources in spectrofluorometers.[8–9] A wide range of wavelengths are available with LEDs (Figure 2.10, see also Figure 4.13). In order

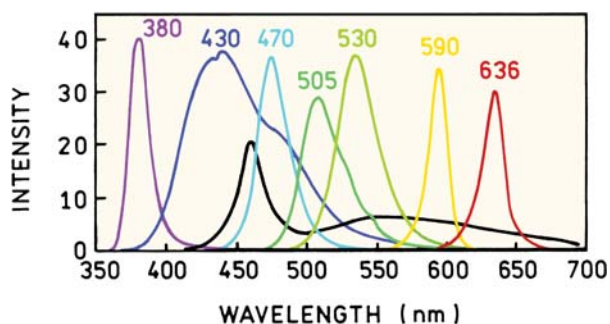**Table 2.1**. Strong Emission Lines from a Mercury–Argon Calibration Source[a]

Mercury lines (nm)			Argon lines (nm)	
253.7	404.7	696.5	763.5	842.5
296.7	407.8	706.7	772.4	852.1
302.2	435.8	710.7	794.8	866.8
313.2	546.1	727.3	800.6	912.3
334.1	577.0	738.0	811.5	922.6
365.0	579.1	750.4	826.5	

[a]Data from [7].

for time-resolved measurements is described in Chapters 4 and 5.

2.3. MONOCHROMATORS

Monochromators are used to disperse polychromatic or white light into the various colors or wavelengths. This dispersion can be accomplished using prisms or diffraction gratings. The monochromators in most spectrofluorometers use diffraction gratings rather than prisms. The performance specifications of a monochromator include dispersion, efficiency, and stray light levels. Dispersion is usually given in nm/mm. The slit width is sometimes expressed in mm, which requires knowledge of the dispersion. A monochromator for fluorescence spectroscopy should have low stray light levels to avoid problems due to scattered or stray light. By stray light we mean light transmitted by the monochromator at wavelengths outside the chosen wavelength and bandpass. Monochromators are also chosen for high efficiency to maximize the ability to detect low light levels. Resolution is usually of secondary importance since emission spectra rarely have peaks with line widths less than 5 nm. The slit widths are generally variable, and a typical monochromator will have both an entrance and exit slit. The light intensity that passes through a monochromator is approximately proportional to the square of the slit width. Larger slit widths yield increased signal levels, and therefore higher signal-to-noise ratios. Smaller slit widths yield higher resolution, but at the expense of light intensity. If the entrance slit of the excitation monochromator is already wide enough to accept the focused image of the arc, then the intensity will not be increased significantly with a wider slit width. If photobleaching of the sample is a problem, this factor can sometimes be minimized by decreasing the excitation intensity. Gentle stirring of the sample can also minimize photobleaching. This is because only a fraction of the sample is illuminated and the bleached portion of the sample is continuously replaced by fresh solution.

to obtain a wide range of wavelengths an array of LEDs can be used.[8] LEDs can be placed close to the samples, and if needed the excitation wavelength can be defined better by the use of an excitation filter. Unlike a xenon lamp, LEDs do not generate significant infrared, so that an additional heat filter is not needed. There are ongoing efforts to develop white LEDs, which are already found in LED flashlights. These LEDs contain phosphors to provide a wider range of wavelengths.[9] LEDs have the advantage of long life and low power consumption. The use of LEDs as an excitation source is likely to broaden in the near future.

2.2.8. Laser Diodes

Another light source is the laser diode. In contrast to LEDs, laser diodes emit monochromatic radiation. Laser diodes are available with wavelengths ranging from about 405 to 1500 nm. Laser diodes are convenient because the output is easily focused and manipulated. In contrast to arc lamps or incandescent lamps, the output of LEDs and laser diodes can be pulsed or modulated. LEDs can be amplitude modulated up to about 100 MHz, and laser diodes can be modulated to several GHz. The use of these light sources
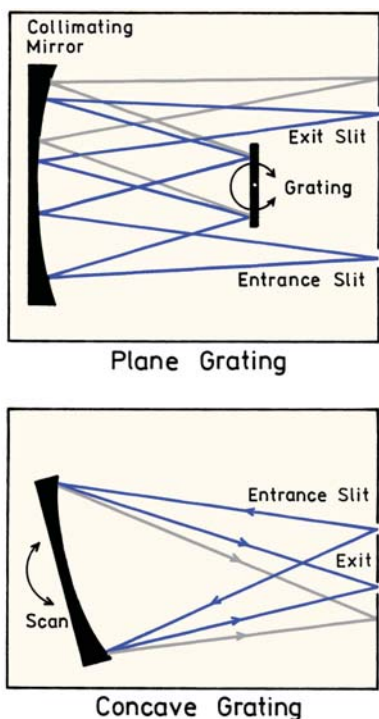
Monochromators can have planar or concave gratings (Figure 2.11). Planar gratings are usually produced mechanically. Concave gratings are usually produced by holographic and photoresist methods. Imperfections of the gratings are a source of stray light transmission by the monochromators, and of ghost images from the grating. Ghost images can sometimes be seen within an open monochromator as diffuse spots of white light on the inside surfaces. Monochromators sometimes contain light blocks to intercept these ghost images. Monochromators based on

Figure 2.10. Spectral output of light-emitting diodes [8]. The black line shows the output of a white LED [7].

Figure 2.11. Monochromators based on a plane (top) or concave (bottom) grating. Revised from [7].

concave gratings can have fewer reflecting surfaces, lower stray light, and can be more efficient. A concave grating can serve as both the diffraction and focusing element, resulting on one instead of three reflecting surfaces. For these reasons the holographic gratings are usually preferable for fluorescence spectroscopy.
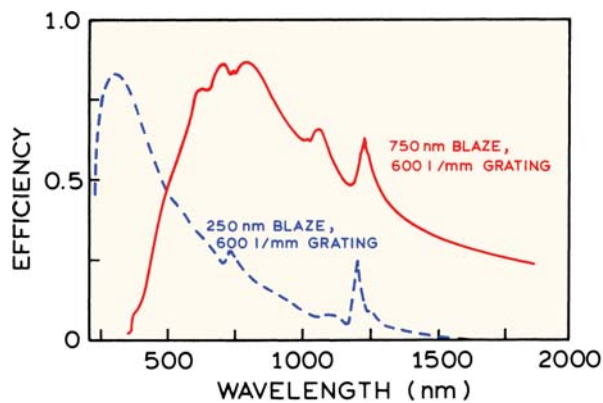
Figure 2.12. Efficiency of two-ruled grating blazed for different wavelengths. Redrawn from [5]. Courtesy of Newport Corp.
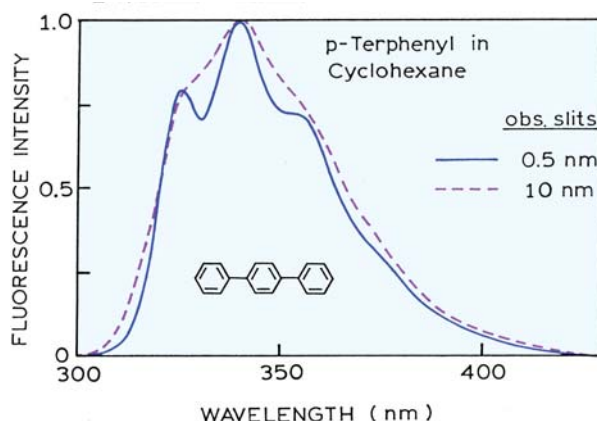

Figure 2.13. Emission spectra of p-terphenyl collected with a spectral resolution of 0.5 and 10 nm. From [10].

The transmission efficiency of a grating and monochromator is dependent on wavelength and on the design of the grating. Examples are shown in Figures 2.12 and 2.13. For a mechanically produced plane grating the efficiency at any given wavelength can be maximized by choice of blaze angle, which is determined by the shape and angle of the tool used to produce the grating. By choice of this angle one may obtain maximum diffraction efficiency for a given wavelength region, but the efficiency is less at other wavelengths. For the examples shown in Figure 2.12 the efficiency was optimized for 250 or 750 nm. Generally, the excitation monochromator is chosen for high efficiency in the ultraviolet and an emission monochromator for high efficiency at visible wavelengths.

2.3.1. Wavelength Resolution and Emission Spectra

The emission spectra of most fluorophores are rather broad and devoid of structure. Hence, the observed emission spectra are typically independent of spectral resolution. For fluorophores that display structured emission, it is important to maintain adequate wavelength resolution, which is adjusted by the slit widths on the monochromator. Emission spectra of p-terphenyl are shown in Figure 2.13. They display vibrational structure when recorded with a resolution of 0.5 nm. However, this structure is nearly lost when the resolution is 10 nm. Although not important for steady-state measurements, the transit time through a monochromator can depend on wavelength (Section 4.6.5).
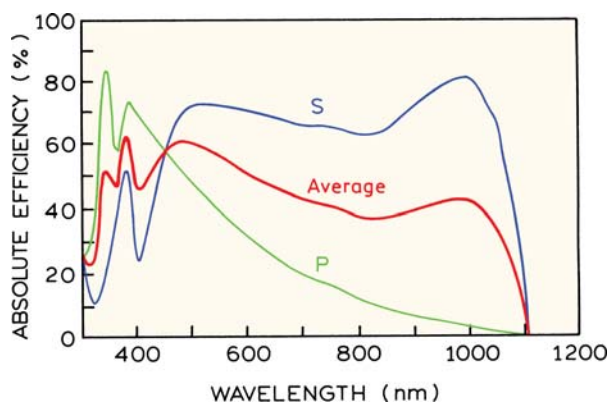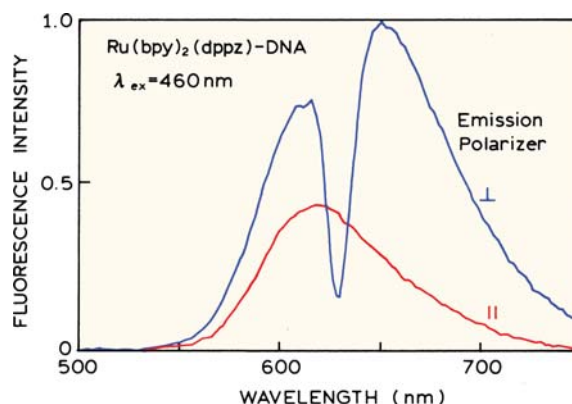
Figure 2.14. Grating efficiency for a 1800 line/mm halographic grating, optimized for the UV. The bold line is the average, and the other lines are for differently (S and P) polarized light, defined in Figure 2.39. Redrawn from [11].

Figure 2.15. Emission spectra of $[Ru(bpy)_2(dppz)]^{2+}$ bound to DNA. This probe is described in chapter 20. Excitation at 460 nm. Except for intensity, the same spectral distributions was observed for vertically as horizontally polarized excitation. From [12].

2.3.2. Polarization Characteristics of Monochromators

For a grating monochromator the transmission efficiency depends upon the polarization of the light. This is illustrated in Figure 2.14 for a concave grating. For this reason, the observed fluorescence intensities can be dependent upon the polarization displayed by the fluorescence emission. The emission spectrum can be shifted in wavelength and altered in shape, depending upon the polarization conditions chosen to record the emission spectrum. For example, consider an emission spectrum recorded with the grating shown in Figure 2.14, and through a polarizer oriented vertically ($\parallel$) or horizontally ($\perp$). Assume that the dotted transmission curve corresponds to vertically polarized light. The spectrum recorded through the vertically oriented polarizer would appear shifted to shorter wavelengths relative to that recorded with the polarizer in the horizontal position. This is because the transmission efficiency for vertically polarized light is higher at shorter wavelengths. This spectral shift would be observed irrespective of whether its emission was polarized or not polarized.

The polarization properties of concave gratings can have a dramatic effect on the appearance of emission spectra. This is shown in Figure 2.15 for a probe bound to DNA. The emission spectrum shows a dramatic decrease near 630 nm when the emission polarizer is in the horizontal position. This drop is not seen when the emission polarizer is in a vertical orientation. In addition to this unusual dip in the spectrum, the emission maximum appears to be different for each polarizer orientation. These effects are due to the polarization properties of this particular grating, which dis-

plays a minimum in efficiency at 630 nm for horizontally polarized light. Such effects are due to the emission monochromator, and are independent of the polarization of the excitation beam.

The polarization characteristics of monochromators have important consequences in the measurement of fluorescence anisotropy. Such measurements must be corrected for the varying efficiencies of each optical component. This correction is expressed as the G factor (Section 10.4). However, the extreme properties of the concave gratings (Figure 2.14) can cause difficulties in the measurement of fluorescence polarization. For example, assume that the polarization is to be measured at an excitation wavelength of 450 nm. The excitation intensities will be nearly equal with the excitation polarizers in each orientation, which makes it easier to compare the relative emission intensities. If the emission is unpolarized the relative intensities with parallel ($\parallel$) and perpendicular ($\perp$) excitation intensities will be nearly equal. However, suppose the excitation is at 340 nm, in which case the intensities of the polarized excitation will be very different. In this case it is more difficult to accurately measure the relative emission intensities because of the larger difference in the excitation intensities. Measurement of the G factor is generally performed using horizontally polarized light, and the intensity of this component would be low.

2.3.3. Stray Light in Monochromators

The stray light level of the monochromator is a critical parameter for florescence measurements. Stray light is

defined as any light that passes through the monochromator besides the desired wavelength. Consider the excitation monochromator. The entire output from the light source enters the monochromator. Ultraviolet wavelengths are frequently used for excitation, and the ultraviolet intensity may be 100-fold less than the visible output of the Xe lamp. Stray light at longer wavelengths can be passed by the excitation monochromator, and can easily be as intense as the fluorescence itself. Fluorescence intensities are frequently low, and many biological samples possess significant turbidity. The incident stray light at the emission wavelength can be scattered, and can interfere with measurements of the fluorescence intensity. For these reasons, double-grating monochromators are frequently used, especially for excitation. Stray light levels for such monochromators are frequently 10^{-8} to 10^{-12} of the peak intensities. However, double-grating monochromators are less efficient, and sensitivity must be sacrificed.

The stray light properties of the emission monochromator are also important. Generally, only a low percentage of the exciting light is absorbed by the fluorophores, and fluorescence quantum yields can be small. It is not unusual for the fluorescence signal to be 1000-fold less intense than the exciting light. Now consider a turbid suspension of membranes, from which we wish to observe the fluorescence of membrane-bound proteins. The excitation and emission wavelengths would be near 280 and 340 nm, respectively. Since the emission monochromator is imperfect, some of the scattered light at 280 nm can pass through the emission monochromator set at 340 nm. Assume that the emission monochromator, when set at 340 nm, discriminates against 280 nm by a factor of 10^{-4}. The intensity of scattered light at 280 nm can easily be 10^3–fold more intense than the fluorescence at 340 nm. Hence 10% of the "fluorescence" at 340 nm may actually be due to scattered exciting light at 280 nm. It is also important to recognize that scattered light is highly polarized, typically 100%. This means that the scattered light will contribute to the vertical intensity but not to the horizontal intensity. Stray scattered light can easily invalidate measurements of fluorescence anisotropy.

The stray light rejection of holographic gratings is superior to that of the mechanically produced ruled gratings. It appears that the passage of stray light depends upon imperfections in the gratings, resulting in ghost images which can escape from the monochromators. Fewer such images are present with the holographic gratings because they are produced optically and have fewer imperfections. In addition, monochromators with holographic gratings generally have fewer reflecting surfaces within the monochromators (Figure 2.11). This is because the concave grating can also act as an imaging device, and thus additional concave mirrors are not required for focusing. With fewer reflecting surfaces there is a decreased probability of stray light escaping from the monochromator.

2.3.4. Second-Order Transmission in Monochromators

Another source of unwanted light is higher-order light diffraction by the monochromator. Light diffraction at the grating can occur as a first, second- or higher-order process. These diffraction orders frequently overlap (Figure 2.16). Suppose the excitation monochromator is set at 600 nm. The xenon light source contains output of both 300 and 600 nm. When the monochromator is set at 600 nm, some 300-nm light can be present at the exit slit due to second-order diffraction.

Transmission of second-order diffraction can also result in extraneous light passing through the emission monochromators. Suppose the excitation is at 300 nm and the emission monochromator is scanned through 600 nm. If the sample is strongly scattering, then some of the scattered light at 300 nm can appear as second-order diffraction when the emission monochromator is set to 600 nm. The emission spectrum from a turbid solution can have a peak at twice the excitation wavelength due to 2nd-order transmission through the emission monochromator. Bandpass excitation filters can be used to remove unwanted wavelengths from the excitation beam.
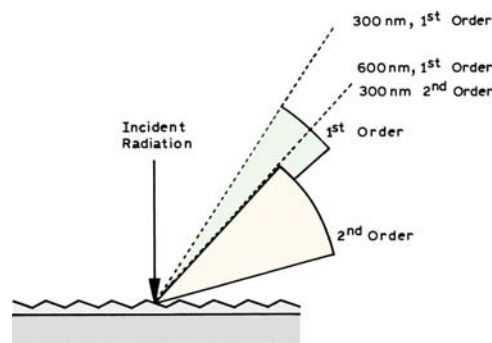
Figure 2.16. First- and second-order diffraction off a diffraction grating. The region where there is no overlap of the 1st- and 2nd-order diffraction is called the free spectral range.

2.3.5. Calibration of Monochromators

The wavelength calibration of monochromators should be checked periodically. Calibration can be performed using a low pressure mercury or mercury–argon lamp. These lamps are shaped like a cylinder, about 5 mm in diameter, and conveniently fit into the cuvette holder. These lamps provide a number of sharp lines that can be used for calibration (Figure 2.9). The lamp can be held stationary with a block of metal in which the lamp fits snugly. This holder is the same size as a cuvette. A pinhole on the side of this holder allows a small amount of the light to enter the emission monochromator. A small slit width is used to increase the precision of wavelength determination and to decrease light intensity. It is important to attenuate the light so that the photomultiplier tube and/or amplifiers are not damaged. Following these precautions, the dominant Hg lines are located using the emission monochromator. The measured wavelengths are compared with the known values, which are listed in Table 2.1. Since there are multiple Hg lines, it is necessary to observe three or more lines to be certain a line is assigned the correct wavelength. If the observed wavelengths differ from the known values by a constant amount, one recalibrates the monochromator to obtain coincidence. A more serious problem is encountered if the wavelength scale is nonlinear.

After calibration of the emission monochromator, the excitation monochromator can be calibrated against this new standard. The slits on both monochromators should be set to the same small value, consistent with the available light intensity. A dilute suspension of glycogen or Ludox is placed in the cuvette holder to scatter the exciting light. The emission monochromator is set to some arbitrary wavelength. If the excitation monochromator is properly calibrated, then the maximum intensity of the scattered light is seen when the indicated wavelengths are identical. The linearity of the wavelength scale can be determined by setting the emission monochromator at various wavelengths. One advantage of this procedure is that there is no need to remove the light source. The mercury light can be used in place of the xenon lamp to calibrate the excitation monochromator, but then the xenon lamp must be removed.

2.4. OPTICAL FILTERS

2.4.1. Colored Filters

While spectrofluorometers have monochromators for wavelength selection, it is often important to use optical filters in
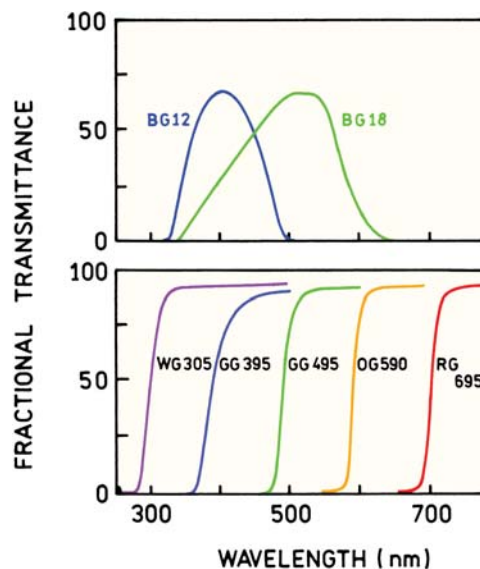
Figure 2.17. Transmission spectra of some typical colored glass filters. From [13].

addition to monochromators. Optical filters are used to compensate for the less-than-ideal behavior of monochromators. Also, when the spectral properties of a fluorophore are known, maximum sensitivity is often obtained using filters rather than monochromators. A large range of filters are available. The manufacturers typically provide the transmission spectra of the filters. Before the advances in thin film technology, most filters were colored-glass filters. Colored-glass filters can transmit a range of wavelengths (Figure 2.17, top). Some color filters are called long-pass filters and transmit all wavelengths above some particular wavelength (bottom). The names of the filters divide them into classes according to their colors (BG, blue glass, GG, green glass, etc.).

The transmission spectra shown in Figure 2.17 are visually pleasing but may not provide all the needed information. In turbid or dilute samples the scattered light can be orders of magnitude more intense than the fluorescence. This is also true for two-photon excitation when the excitation wavelength is longer than the emission wavelength. For these reasons transmission curves are often presented on a logarithm scale, which makes it possible to determine if the filter transmits 1% or much less than 1% of the light at any given wavelength (Figure 2.18). These curves also show transmission at longer wavelengths, where there may be interference from scattered light from the higher-order transmission of monochromators.
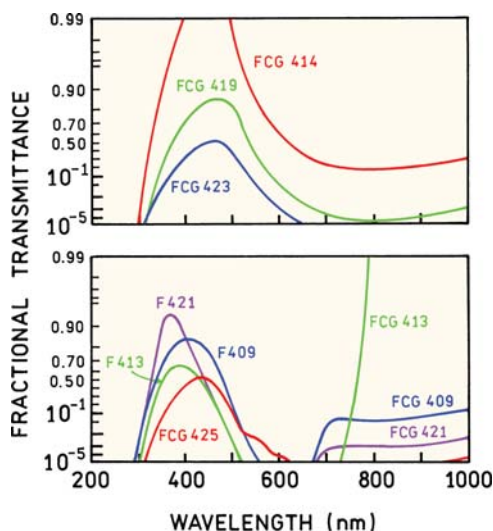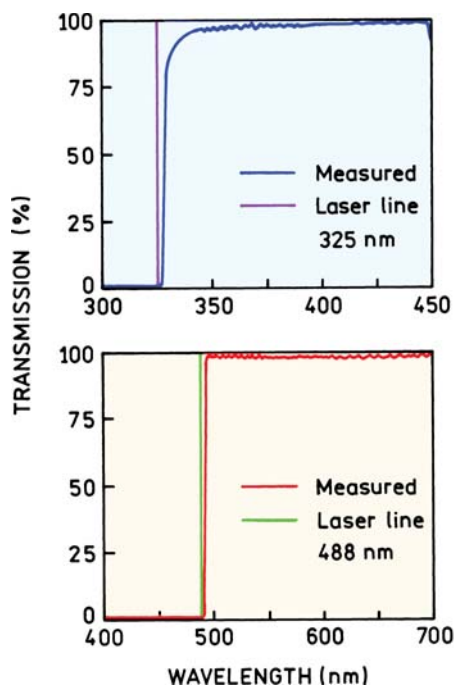
Figure 2.18. Transmission spectra of colored-glass filters. Top: in order of increasing wavelength FCG 414, 419, and 423. Bottom: FCG 409, 413, 421, and 425. From [13].

Figure 2.19. Long-pass filters designed to reject light from a helium-cadmium laser at 325 nm or an argon ion laser at 488 nm. Revised from [15].

An important consideration in the use of bandpass filters is the possibility of emission from the filter itself. Many filters are luminescent when illuminated with UV light, which can be scattered from the sample. For this reason it is usually preferable to locate the filter further away from the sample, rather than directly against the sample. Glass filters of the type shown in Figures 2.17 and 2.18 are highly versatile, effective, and inexpensive, and a wide selection is needed in any fluorescence laboratory. Excitation and emission filters can be used in all experiments, even those using monochromators, to reduce the possibility of undesired wavelengths corrupting the data.

2.4.2. Thin-Film Filters

A wide variety of colored-glass filters are available, but the transmission curves are not customized for any given application. During the past ten years there have been significant advances in the design of thin-film optical filters.[14] Almost any desired transmission curve can be obtained. Filters are now being designed for specific applications, rather than choosing the colored-glass filter that best suits an application. Long-pass filters are an example of this type filter (Figure 2.19). These filters have a sharp cut on the transmission above 325 nm or 488 nm, which are wavelengths available from a helium–cadmium or argon ion laser, respectively. The transmission above the cut-on wavelength is close to 100% to provide maximum sensitivity.

Thin-film filters are also available to specifically transmit or reject laser lines. Laser light can contain additional wavelengths in addition to the main laser line. This emission is referred to as the plasma emission, which typically occurs over a range of wavelengths and is not strongly directional. The light can be made more monochromatic by passing the laser beam through a laser line filter, such as the one shown for a helium–neon laser at 633 nm (Figure 2.20). Alternatively, it may be necessary to eliminate scattered light at the laser wavelength. This can be accomplished with a notch filter which transmits all wavelengths except the laser wavelengths. These filters are sometimes called Raman notch filters because of their use in Raman spectroscopy.

Emission can usually be selected using a long-pass filter. However, there may be additional emission at longer wavelengths, such as the acceptor emission in an energy transfer experiment. In these cases it is useful to have a filter that transmits a selected range of wavelengths or autofluorescence from the sample. Figure 2.21 shows examples of bandpass filters that transmit from 460 to 490 nm or from 610 to 700 nm. The width of transmission can be made narrower or wider. Such filters are often referred to as interference filters.
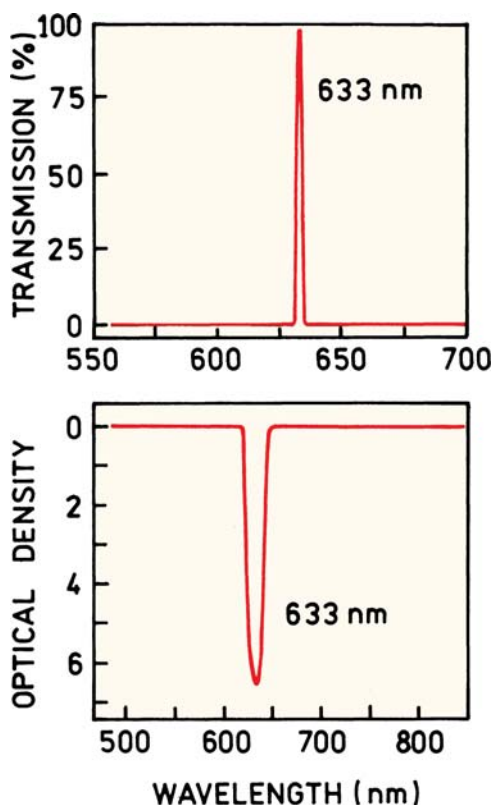
Figure 2.20. Laser line filter to transmit only the laser wavelength (top) and a notch filter to reject the laser wavelength. From [15].
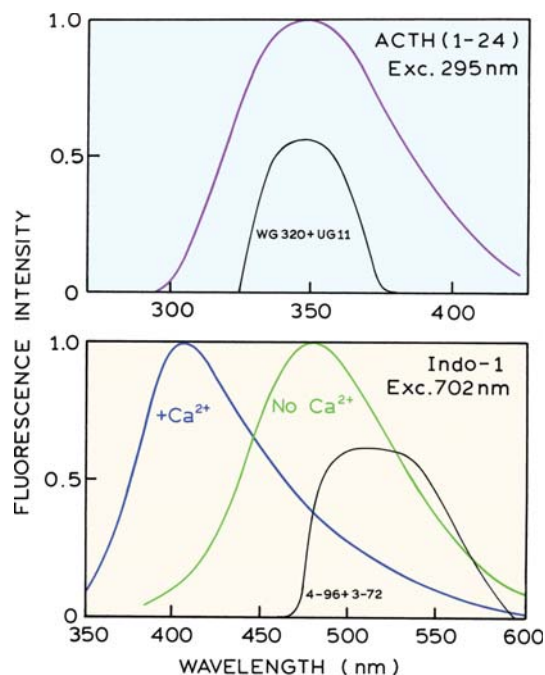
2.4.3. Filter Combinations

While one can obtain almost any desired filter with modern coating technology, the design of custom filters for each experiment is usually not practical. If a single filter is not
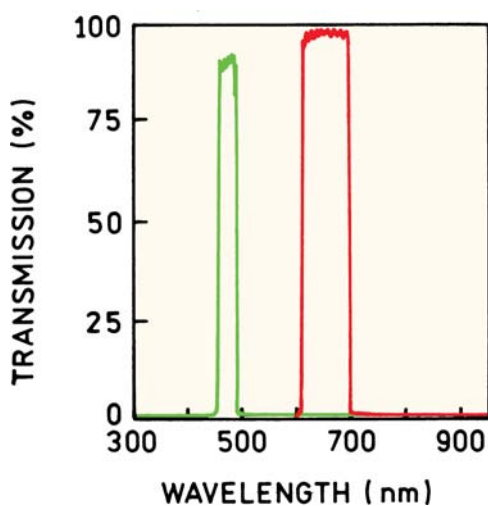
Figure 2.21. Interference filter to transmit selected wavelengths. From [15].

Figure 2.22. Transmission profile of a combination of Corning and Schott filters used to isolate protein fluorescence (top) and Indo-1 fluorescence (bottom). Lower panel from [17].

adequate for a given experiment, it is often possible to combine two or more bandpass filters to obtain the desired spectral properties. This possibility is shown in Figure 2.22. The UG-11 and WG-320 filters are often used in our laboratory to isolate protein fluorescence.[16] For probes emitting near 450 nm, we often use a combination of Corning 4-96 and 3-72 filters.[17] In this example the filter was selected to reject 702 nm, which was the excitation wavelength for two-photon excitation of Indo-1.[17] This example illustrates an important aspect in selecting filters. Filters should be selected not only for their ability to transmit the desired wavelength, but perhaps more importantly for their ability to reject possible interfering wavelengths.

2.4.4. Neutral-Density Filters

Neutral-density filters are used to attenuate light equally at all wavelengths. They are typically composed of sheets of glass or quartz coated with a metal to obtain the desired optical density. Quartz transmits in the UV and is preferred unless no experiments will be done using wavelengths below 360 nm. Neutral-density filters are described by their optical density, and can typically be obtained in increments of 0.1, up to optical densities of 4. It is often necessary to adjust or match the intensity of two signals, which is conveniently accomplished using neutral-density filters.
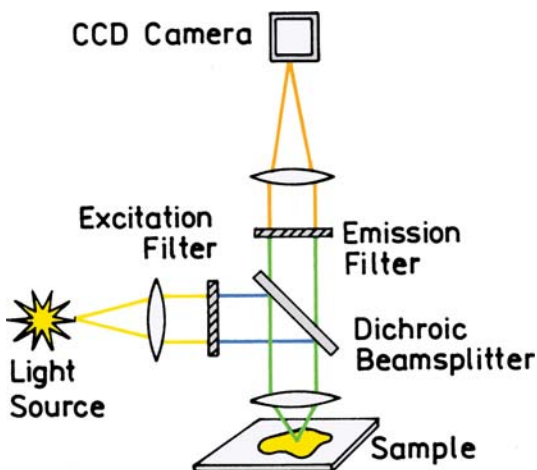
Figure 2.23. Filter geometry used for epifluorescence microscopy.

2.4.5. Filters for Fluorescence Microscopy

Fluorescence microscopy relies on optical filters rather than monochromators for wavelength selection. Most fluorescence microscopy is performed using the epifluorescence configuration. The term epifluorescence refers to excitation and emission passing through the same objective (Figure 2.23). This configuration has the advantage of most of the excitation traveling away from the detector. Additionally, the excitation can be observed for the same location. Even though most of the excitation passes through the sample, a substantial fraction of the excitation is reflected or scattered back into the objective.

Observation of the fluorescence image requires specially designed sets of filters. A set contains an excitation filter, an emission filter, and a dichroic beam splitter. The function of such filters can be understood by examination of their transmission spectra (Figure 2.24). The excitation filter selects a range of wavelengths from a broadband source to excite the sample. The emission filter transmits the emission and rejects the excitation wavelengths. The unusual component is the dichroic beam splitter, which serves a dual function. It reflects the excitation wavelengths into the objective, and transmits the emission and allows it to reach the eyepiece or detector. Filter sets for microscopy are now often named for use with specific fluorophores rather than wavelengths.

Fluorescence microscopy is often performed using multiple fluorophores to label different regions of the cell, allowing the region to be identified by the emission wavelength. Emission filters have been designed to pass the emission from multiple fluorophores. Figure 2.25 shows
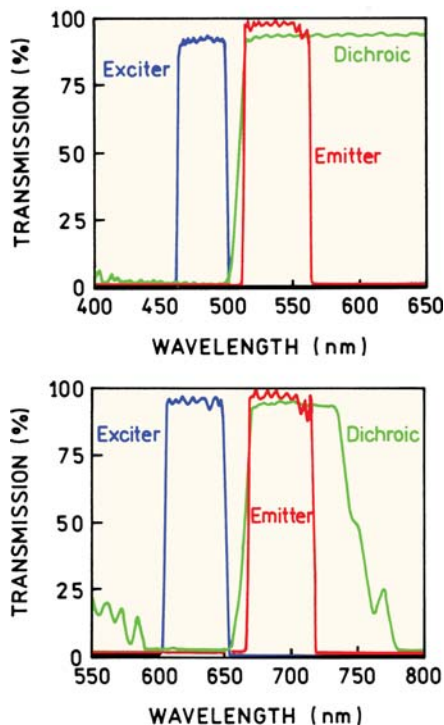

Figure 2.24. Epifluorescence filter sets for fluorescein or Cy5. From [15].
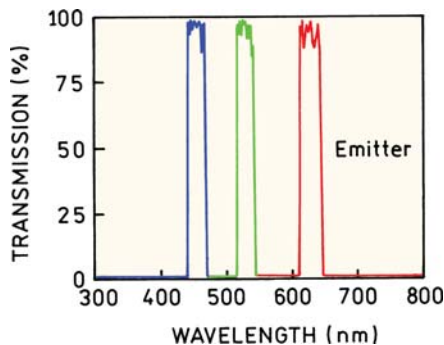

Figure 2.25. Multi-bandpass filter designed to transmit the emission of DAPI, fluorescein and Texas Red. Note that this is a single filter with three bandpasses. From [15].

the transmission curve of a filter designed to pass the emission from DAPI near 460 nm, fluorescein near 530 nm, and Texas Red at 630 nm. The availability of such filters has greatly expanded the capabilities of fluorescence microscopy.

2.5. OPTICAL FILTERS AND SIGNAL PURITY

A major sources of errors in all fluorescence measurements is interference due to scattered light, stray light, or sample
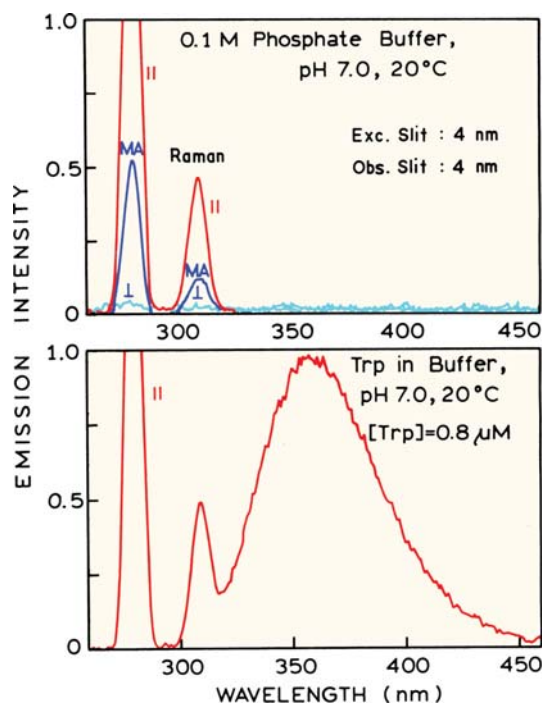
Figure 2.26. Emission spectrum of a 0.8-μM solution of tryptophan (bottom) in 0.1 M phosphate buffer, pH 7.0. The observation polarizer was vertically oriented. Top: emission spectrum of a blank buffer solution under the same optical conditions. The emission polarizer was vertical (∥), horizontal (⊥) or at the 54.7° magic angle (MA) position. From [10].

impurities. These problems can be minimized by careful selection of the emission filter, the use of optical filters in addition to the excitation and emission monochromators, and by control experiments designed to reveal the presence of unwanted components. The use of optical filters and control experiments to avoid such artifacts is best illustrated by specific examples.

Figure 2.26 (bottom) shows the emission spectrum of a dilute solution of tryptophan in aqueous buffer. The large sharp peak on the left is due to scattered excitation, the broad peak at 360 nm is the tryptophan fluorescence, and the small sharp peak at 310 nm is the Raman scatter. Raman scatter will occur from all solvents. For water, the Raman peak appears at a wavenumber 3600 cm^{-1} lower than the incident wavenumber. For excitation at 280 nm, the Raman peak from water occurs at 311 nm. Highly fluorescent samples generally overwhelm the Raman peak. However, if the gain of the instrument is increased to compensate for a dilute solution or a low quantum yield, the Raman scatter may become significant and distort the emission spectrum. Raman scatter always occurs at a constant wavenumber dif-

ference from the incident light, and can be identified by changing the excitation wavelength. Also, the spectral width of the Raman peak will be determined by the resolution of the monochromators.

In microscopy and in assays the fluorescence may be observed without a monochromator. The emission can be observed through a filter that is presumed to remove the scattered light. Observation through a filter rather than a monochromator increases the sensitivity because the bandpass of the observation is increased and the attenuation due to the monochromator is removed. The signal level can often be 50-fold higher when observed through filters rather than a monochromator. Lifetime measurements are usually performed using long-pass filters to observe the entire emission. Under these conditions it is important to choose an emission filter that eliminates both the scattered incident light and the Raman scatter.

In any fluorescence experiment it is essential to examine blank samples, which are otherwise identical to the sample but do not contain the fluorophore. These control samples allow the presence of Rayleigh and Raman scatter to be determined. Control samples can also reveal the presence of fluorescent impurities. An emission spectrum of the buffer blank for the dilute tryptophan solution is shown in Figure 2.26 (top). The gain of the instrument should be the same when recording the emission spectrum of the sample and that of the blank. These control spectra are recorded under the same conditions, because the only meaningful consideration is whether the blank contributes to the emission under the conditions of a given experiment. In this case the blank spectrum above 320 nm is essentially zero, showing that the peak at 360 nm (bottom) is in fact due to the sample. While this may seem like a trivial result, the presence of background fluorescence and/or scattered light is the most common error in fluorescence measurements. Examination of the blank sample also allows identification of the peak at 310 nm as due to the buffer and not to the sample.

The most appropriate blank solution is one that is identical to the sample, but does not contain the fluorophore. This can be difficult to accomplish with protein or membrane solutions, where the macromolecules themselves are the source of the signal. Such solutions will typically be more strongly scattering than the buffer blanks. In these cases it is useful to add glycogen or colloidal silica (Ludox) to the buffer blank, to mimic the amount of scattering from the sample. This allows selection of filters that are adequate to reject scattered light from the sample.
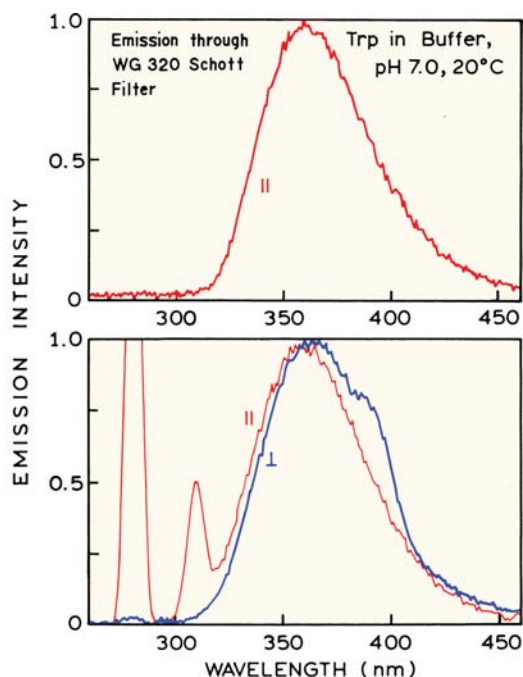
Figure 2.27. Rejection of scattered light from the 0.8-μM tryptophan solution using a bandpass filter (top) or a polarizer but no bandpass filter (bottom). The emission polarizer was oriented vertically (‖) or horizontally (⊥). From [10].

2.5.1. Emission Spectra Taken through Filters

Suppose you wanted to measure the lifetime of the tryptophan sample in Figure 2.26 (bottom) and the measurements are to be performed using a bandpass filter to isolate the emission. How can one know the scattered light has been rejected by the emission filter? This control is performed by collecting an emission spectrum through the filter used to measure the lifetime (Figure 2.27, top). In this case the Schott WG320 filter rejected both the scattered light and the Raman scatter, as seen by the zero intensity from 280 to 310 nm. In some cases the filter itself can be a source of background emission. The use of an equivalent scattering solution is preferred, as this provides the most rigorous test of the filter for rejecting scattered light and for displaying minimal fluorescence.

It is important to remember that scattered light is usually 100% polarized ($p = r = 1.0$). This is the reason the emission polarizer was vertical in Figure 2.27 (top), which is the worst-case situation. If the emission spectrum was recorded with the polarizer in the horizontal position, then the scattered light would be rejected by the polarizer (Figure 2.27, bottom). If the sample is then measured with a vertical polarizer, scattered light may be detected. When examining spectra for the presence of scattered light, it is preferable to keep both polarizers in the vertical position, and thereby maximize the probability that the interfering signal will be observed. Conversely, a horizontal emission polarizer can be used to minimize the scattered light if only the emission spectrum needs to be recorded.

The emission spectra in Figure 2.27 (bottom) illustrate how the polarization-dependent transmission properties of the monochromator can distort the emission spectra. For these spectra the excitation was polarized vertically, and the emission spectra were recorded through a polarizer oriented vertically (‖) or horizontally (⊥). These spectra are clearly distinct. The spectrum observed through the vertically oriented polarizer is blue shifted relative to the spectrum observed when the emission polarizer is in the horizontal orientation. The extra shoulder observed at 390 nm is due to the transmission properties of the monochromator. These results illustrate the need for comparing only those spectra that were recorded under identical conditions, including the orientation of the polarizers. The emission spectra for the same fluorophore can differ slightly if the emission is polarized or unpolarized.

One way to avoid these difficulties is to use a defined orientation of the polarizers when recording emission spectra. One preferred method is to use the so-called "magic angle" conditions. This is vertically polarized excitation and an emission polarizer oriented 54.7° from the vertical. In effect, the use of this condition results in a signal proportional to the total fluorescence intensity (I_T) which is given by $I_‖ + 2I_⊥$, where $I_‖$ and $I_⊥$ are the intensities of vertically and horizontally polarized emission. Such precautions are generally taken only when necessary. If the excitation source is unpolarized, the presence of polarizers in both the excitation and emission light paths results in an approximate fourfold decrease in signal level.

Polarization or anisotropy measurements are frequently performed using filters rather than monochromators. Scattered light is 100% polarized ($r = 1.0$). Hence, a small percentage of scatter can result in serious errors. For example, assume 10% of the observed intensity is due to Raman scatter. Furthermore, assume that the actual anisotropy of a sample, in the absence of scatter, is 0.10. The observed anisotropy is then given by

$$r_{obs} = f_s r_s + f_F r_F \tag{2.1}$$

where the f_s value represents the fractional contribution of the scattered light, f_F is the fractional contribution of the flu-
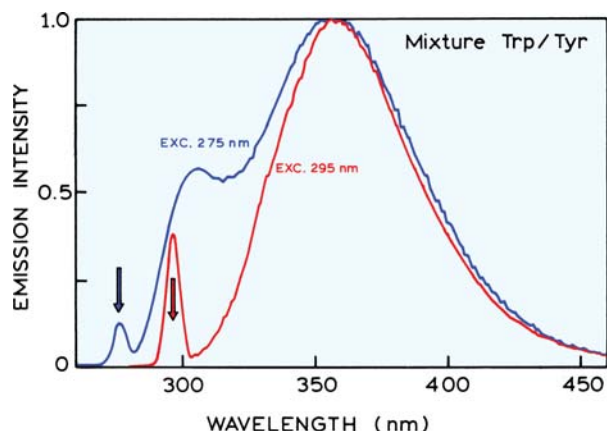
Figure 2.28. Emission spectra of tryptophan with a trace impurity of tyrosine, for excitation at 275 and 295 nm. From [10].

Figure 2.29. Schematic diagram of a photomultiplier tube and its dynode chain.

orescence, r_F is the anisotropy of the fluorescence, and r_s is the anisotropy of the scattered light. Substitution into eq. 2.1 yields $r_{obs} = 0.19$. Hence, a 10% contribution from scattered light can result in an almost twofold error in the measured anisotropy. The relative error would be still larger if r_F was smaller. These considerations apply to both Raman and Rayleigh scattering.
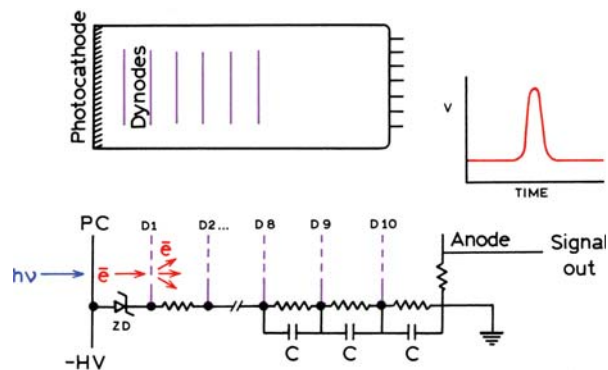
When measuring tryptophan or protein emission it is important to recognize that Raman scatter can be mistaken for tyrosine emission. This possibility is shown in Figure 2.28, which shows the emission spectrum of a tryptophan solution that contains a minor amount of tyrosine. Upon excitation at 275 nm the tyrosine results in a peak near 300 nm. The fact that this peak is due to tyrosine is shown by the spectrum obtained for 295-nm excitation, which shows only the tryptophan emission. If the emission spectrum of tryptophan alone was recorded at lower resolution, one can readily imagine how the broadened Raman line would become visually similar to tyrosine emission (Figure 2.28).

2.6. PHOTOMULTIPLIER TUBES

Almost all fluorometers use photomultiplier tubes (PMTs) as detectors, and it is important to understand their capabilities and limitations. A PMT is best regarded as a current source. The current is proportional to the light intensity. A PMT responds to individual photons, and the pulses can be detected as an average signal or counted as individual photons.

A PMT vacuum tube consists of a photocathode and a series of dynodes which are the amplification stages (Figure 2.29). The photocathode is a thin film of metal on the inside of the window. Incident photons cause electrons to be ejected from this surface. The generation efficiency of photoelectrons is dependent upon the incident wavelength. The photocathode is held at a high negative potential, typically –1000 to –2000 volts. The dynodes are also held at negative potentials, but these potentials decrease toward zero along the dynode chain. The potential difference between the photocathode and the first dynode potential is generally fixed at a constant voltage by a Zener diode, at values ranging from –50 to –200 volts. This potential difference causes an ejected photoelectron to be accelerated toward the first dynode. Upon collision with the first dynode the photoelectron causes 5 to 20 additional electrons to be ejected, depending on the voltage difference to this dynode. This process continues down the dynode chain until a current pulse arrives at the anode. The size of this pulse depends upon the overall voltage applied to the PMT. Higher voltages result in an increased number of electrons ejected from each dynode, and hence higher amplification. PMTs are useful for low-level light detection because they are low-noise amplifiers. Little additional noise is created as the electrons pass through the PMT. Amplification outside of the PMT generally results in more noise being added to the signal.

For quantitative measurements, the anode current must be proportional to the light intensity. A nonlinear response can result from an excessive current being drawn from the photocathode. Under high-intensity illumination the electrical potential of the photocathode can be decreased because of its limited current-carrying capacity. This decreases the voltage difference between the photocathode and the first dynode, and also decreases the gain. Excessive photocurrents can damage the light-sensitive photocathodes, result-
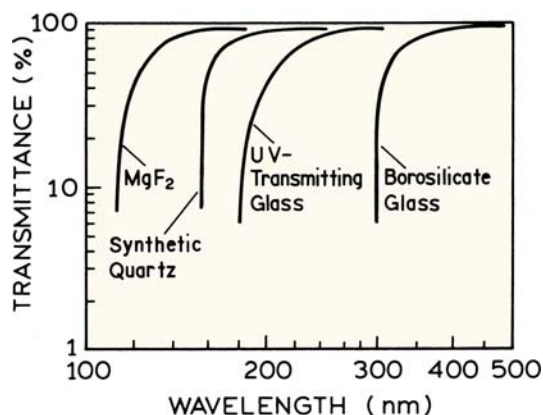
Figure 2.30. Typical transmittance of PMT window materials.

ing in loss of gain and excessive dark currents. The dark current from a PMT is the current in the absence of incident light.

A linear response also requires that the dynode voltages remain constant, irrespective of the incident light level and anode current. Dynode chains are designed so that the total current through the chain is at least 100-fold greater than the maximum anode current. Consider the 10-stage tube shown in Figure 2.29. Using resistors with $R = 100$ kΩ, the dynode current would be 1.0 Ma at 1000 volts total voltage across the PMT. Hence 10 µA should be the maximum anode current. There are often capacitors placed between the higher-numbered dynodes to provide a source of current during a single photoelectron pulse or periods of high illumination. Constant amplification by a PMT requires careful control of the high voltage. A typical PMT will yield a threefold increase in gain for each 100 volts. Hence, a small change in voltage can result in a significant change in the signal. The high voltage supply needs to provide a constant, ripple-free voltage that is stable for long periods of time. Photomultiplier tubes are available in a wide variety of types. They can be classified in various ways, such as according to the design of the dynode chain, size, and shape, spectral response, or temporal response.

2.6.1. Spectral Response of PMTs

The sensitivity of a PMT depends upon the incident wavelength. The spectral response is determined by the type of transparent material used for the window, and the chemical composition of the photocathode. Only light that enters the PMT can generate photocurrent. The input windows must be transparent to the desired wavelengths. The transmission

curves of typical windows material are shown in Figure 2.30. UV transmitting glass is frequently used and transmits all wavelengths above 200 nm. Synthetic quartz can be used for detection deeper into the UV. MgF_2 windows are only selected for work in the vacuum ultraviolet. Since atmospheric oxygen absorbs strongly below 200 nm, there is little reason for selecting MgF_2 unless the apparatus is used in an oxygen-free environment. For this reason the spectral region below 200 nm is called the vacuum ultraviolet.

The second important factor is the material used for the photocathode. Numerous types of photocathodes are available, and the spectral responses of just a few are shown in Figure 2.31. The quantum efficiency is not constant over any reasonable range of wavelengths. This is one origin of the nonideal wavelength response of spectrofluorometers. Most photocathodes are sensitive in the UV, blue and green (300–500 nm) regions of the spectrum. The differences in photocathode material are important mostly for wavelengths above 600 nm. One of the most commonly used is the bialkali photocathode (Figure 2.31), which provides high sensitivity and low dark current. One disadvantage of the bialkali photocathode is the rapid decrease in sensitivity above 600 nm. Given the current emphasis on red and
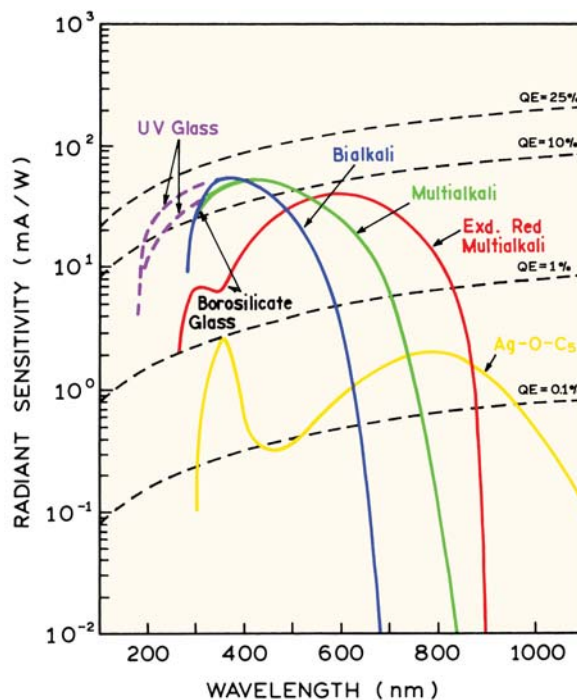

Figure 2.31. Spectral response curves of typical photocathodes. From [18].

Table 2.2. Characteristics of Typical Photomultiplier Tubes[a]

Type	R446 Side window	R2560 Head-on	R3809 Head-on	R3811 Subminiature
Dynode chain	Circular cage	Linear plate	Microchannel cage	Circular cage
Photocathode	Multi-alkali	Bialkali	Multi-alkali S-20	Multi-alkali
Wavelength range (nm)	185–870	300–650	160–185	185–850
Amplification	5×10^6	6×10^6	2×10^5	1.3×10^6
Rise time (ns)	2.2	2.2	0.15	1.4
Transit time (ns)	22	26	0.55	15
Bandwidth (MHz) (estimate)	200	200	2000	300

[a] The number refers to types provided by Hammamatsu Inc.[18]

NIR fluorescence, the bialkali photocathode is becoming less useful.

The sensitivity above 500 nm has been increased by the introduction of multi-alkali and extended red multi-alkali photocathodes, which provide good sensitivity to 700 or 800 nm (Figure 2.31). Red-sensitive PMTs typically have higher dark current, but for most multi-alkali photocathodes the dark current is not a problem. Sensitivity to still longer wavelengths can be obtained using Ag–O–Cs or S-1 photocathodes. However, their quantum efficiency is uniformly poor, and it is often difficult to detect the signal above the dark current with an S-1 PMT. In fact, these PMTs are rarely used without cooling to reduce the dark current.
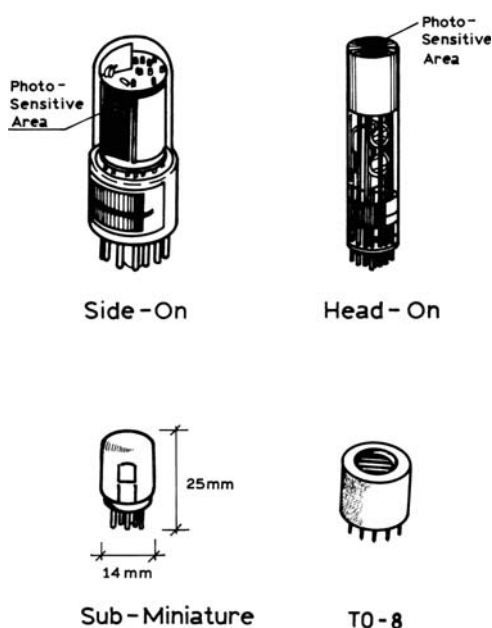
2.6.2. PMT Designs and Dynode Chains

The major types of PMTs and dynode chains used in fluorescence are shown in Figures 2.32 and 2.33. A commonly used PMT is the side-window or side-on tube. A large number of variants are available, and all are descendants of one of the earliest PMTs, the 1P-28. These side-on tubes used a circular cage dynode chain, sometimes referred to as a squirrel cage (Figure 2.33). The specifications of one side-on tube are listed in Table 2.2. The multi-alkali photocathode of the R446 is sensitive from 185 to 870 nm. This type of circular cage PMT has evolved into the subminiature PMTs. Because of their compact design the time response is excellent (Table 2.2). PMTs are also available in the compact TO-8 format, which is 16 nm in diameter. Small PMTs are available complete with a high voltage supply and dynode chain, all in a compact package. These compact high-sensitivity detectors have appeared in many research and clinical instruments.
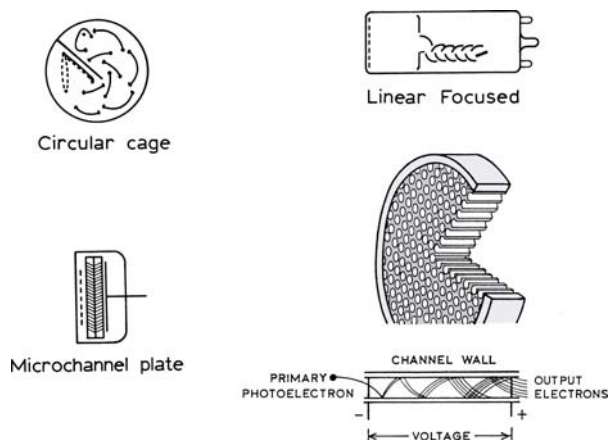

Figure 2.32. Types of photomultiplier tubes.

**Figure 2.33**. Types of PMT dynode chains. From [14].

Another type of PMT is the head-on design (Figure 2.32). This design is used with various types of dynode chains, such as the box and grid, blind and mesh design. For time-resolved fluorescence the head-on PMTs typically use a linear-focused dynode chain (Figure 2.33). The purpose of this design is to minimize the transit time spread and thus improve the time response of the PMT. The use of a head-on design allows the dynode chain to be extended as long as desired, so that the highest amplification is usually available with this type of PMT.

The final type of PMT is the microchannel plate PMT (MCP-PMT). In place of a dynode chain the MCP-PMT has plates that contain numerous small holes (Figure 2.33). The holes in these plates are the microchannels, which are lined with a secondary emissive dynode material. The electrons are amplified as they drop down the voltage gradient across the microchannel plate. Because of the short distances for electron travel, and the restricted range of electron paths, this type of PMT shows the fastest time response and is used in the most demanding time-resolved measurements. MCP-PMTs are available with one, two, or three stages of microchannel plates. The amplification is generally lower than for PMTs with discrete dynode chains. Also, the maximum photocurrent is typically 100 nA, as compared with 10 to 100 μA for a dynode PMT.

2.6.3. Time Response of Photomultiplier Tubes

For steady-state measurements the time response of a PMT is not important. The PMT time response is important for lifetime measurements. There are three main timing characteristics of PMT—the transit time, the rise time, and the transit time spread (Figure 2.34). The transit time of a PMT is the time interval between the arrival of a photon at the cathode and the arrival of the amplified pulse at the anode. Typical transit times range from 20 to 50 ns. The rise time is the time required for the PMT anode signal to rise from 10 to 90% of its final level. The rise time is determined primarily by the transit time variation in the PMT, that is, the scatter around the average transit time.

The transit time spread is the most important specification for time-resolved measurements. These timing variations result from the different geometric paths that the electrons can take from the photocathode to the anode. The photoelectrons can originate from different parts of the photocathode, or can have different trajectories from the same region of the photocathode. The electrons subsequently ejected from the dynodes can take slightly different geo-
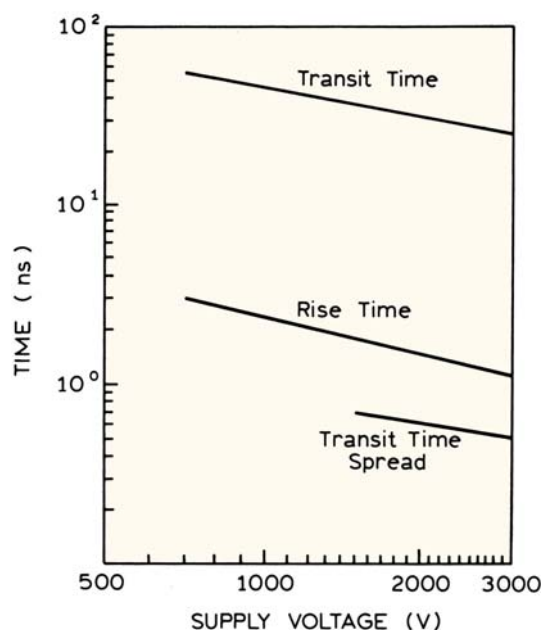
Figure 2.34. Time response of a typical PMT. The data are for a R2059, head on, 12-stage linear focused PMT. Revised from [18].

metric paths through the PMT. This can be seen in Figure 2.29 from the various ejection angles of electrons coming off the first dynode. Transit time spread can be decreased by using photocathode and dynode geometries which minimize the number of different trajectories. This can be accomplished by the use of small illuminated areas, or a dynode designed to direct the flight of the electrons along a defined trajectory.

The most dramatic advance in high-speed PMTs has been the introduction of the MCP-PMT. In this case the photoelectrons are proximity focused into the MCP (Figure 2.33). There is very little variation in terms of electron trajectory within the MCP. For this reason MCP-PMTs have transit time spreads tenfold smaller than those of standard PMTs (Table 2.2).

A second source of the time dependence of a PMT results from the photocathode itself. Typically, its time response is dependent upon the wavelength incident on the photocathode. This property is called the color effect. The energy of the ejected electrons is dependent upon the incident wavelength, and the energy affects the path an electron takes through the phototube. Color effects are not important for steady-state measurements. Color effects were a significant source of error in lifetime measurements, but color effects seem to be smaller in the current generation of fast PMTs.
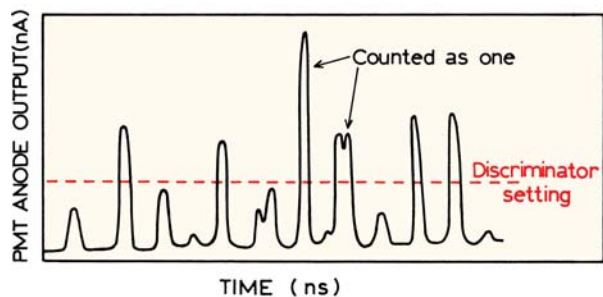
Figure 2.35. Photon-counting detection using a PMT. From [19].

2.6.4. Photon Counting versus Analog Detection of Fluorescence

A PMT is capable of detecting individual photons. Each photoelectron results in a burst of 10^5 to 10^6 electrons, which can be detected as individual pulses at the anode (Figure 2.35). Hence, PMTs can be operated as photon counters, or can be used in the analog mode in which the average photocurrent is measured. Note that we are considering steady-state measurements. Time-correlated photon counting for lifetime measurements will be discussed in Chapter 4. In photon-counting mode, the individual anode pulses due to each photon detected and counted. As a result, the detection system is operating at the theoretical limits of sensitivity. Noise or dark current in the PMT frequently results from electrons that do not originate at the photocathode, but from further down the dynode chain. Such anode pulses from these electrons are smaller, and can be ignored by setting the detection threshold high enough to count only fully amplified primary photoelectrons. Besides increased sensitivity, the stability of the detection system can be increased. Because the PMT is operated at a constant high voltage, small drifts in the voltage do not result in significant changes in the efficiency with which each photon is counted. Photon-counting detection is frequently used when signal levels are low, and when it is necessary to average repetitive wavelength scans to increase the signal-to-noise ratio.

There can be disadvantages to photon counting for steady-state measurements. The gain of the PMT cannot be varied by changing the applied voltage. Photon-counting detection can be inconvenient when signal levels are high. To stay within the linear range, one must adjust the slit widths or the fluorescence intensities (using neutral-density filters). Another disadvantage of photon counting is the limited range of intensity over which the count rate is linear. If

two pulses arrive at the anode closely spaced in time, they will be counted as a single pulse. Anode pulses resulting from a single photon are typically 5 ns wide. This limits the response of the PMT to 200 MHz, or 2×10^8 Hz for a periodic signal. For random events, the count rates need to be about 100-fold less to avoid the simultaneous arrival of two photons. Hence, count rates are limited to several MHz. Manufacturers often specify count rates of 50 MHz or higher. However, these count rates apply to uniformly spaced pulses, and the pulse widths of the detector may be too wide to distinguish pulses which occur too close together. In practice, the count rates often become sublinear before the theoretical upper limit is reached (Figure 2.36). Higher count rates can be obtained with PMTs which show shorter pulse widths. Additionally, the signal-to-noise ratio becomes unsatisfactory at count rates below 10,000 photons per second. The linear dynamic range can be as small as 3 log units (Figure 2.36).[20] This limited intensity range is a drawback of photon-counting detection for steady-state measurements of fluorescence, unless the highest sensitivity is required.

In analog mode the individual pulses are averaged. Since the current from each pulse contributes to the average anode current, the simultaneous arrival of pulses is not a problem. When using analog detection the gain of the detection system can be varied by changing either the amplifier gain or the voltage on the photomultiplier tube. As a result, a wider range of signal levels can be detected without concerns about a nonlinear response. The precision of the individual measurements can be higher than for photon counting measurements, because of the higher overall sig-
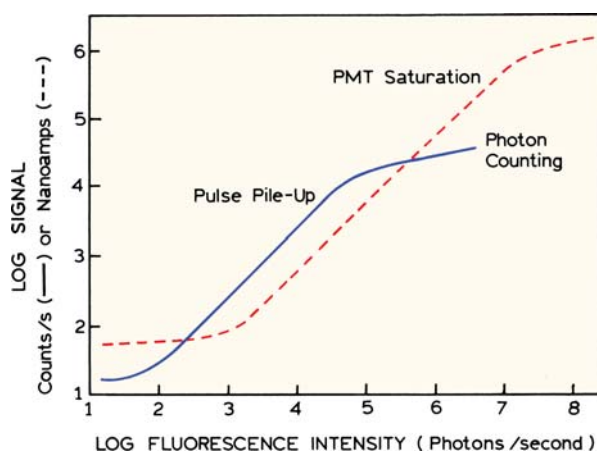

Figure 2.36. Dynamic range available with photon counting and analogue detection. From [19].

nal levels. However, even the analog measurements have a limited range because all PMTs display saturation above a certain light level if one exceeds the capacity of the photocathode to carry the photocurrent, or an ability of the dynode chain to maintain a constant voltage.

2.6.5. Symptoms of PMT Failure

Photomultiplier tubes should be handled with care. Their outer surfaces should be free of dust and fingerprints, and should not be touched with bare hands. The photocathode is light sensitive, and it is best to perform all manipulations in dim light. It is convenient to know the common signs of PMT failure. One may observe pulses of current when the applied voltage is high. At lower voltages this symptom may appear as signal instability. For instance, the gain may change 20% to several-fold over a period of 2–20 seconds. The origin of this behavior is frequently, but not always, a leakage of gas into the tube. The tube cannot be fixed and replacement is necessary. In some instances the tube may perform satisfactory at lower voltages.

A second symptom is high dark current. This appears as an excessive amount of signal when no light is incident on the PMT. The origin of high dark currents is usually excessive exposure of the tube to light. Such exposure is especially damaging if voltage is applied to the tube at the same time. Again, there is no remedy except replacement or the use of lower voltages.

Signal levels can be unstable for reasons other than a failure of the photomultiplier tube. If unstable signals are observed one should determine that there are no light leaks in the instrument, and that the high voltage supplies and amplifiers are functioning properly. In addition, the pins and socket connections of the PMT should be checked, cleaned, and tightened, as necessary. Over a period of years, oxide accumulation can result in decreased electrical contact. Photobleaching of a sample may give the appearance of an instrument malfunction. For example, the fluorescence intensity may show a time-dependent decrease due to bleaching, and then an increase in intensity due to convection currents which replenish the bleached portion of the sample.

2.6.6. CCD Detectors

There is a growing usefulness of charge-coupled devices (CCDs) in fluorescence spectroscopy.[21–22] CCDs are imaging detectors with remarkable sensitivity and linear dynam-
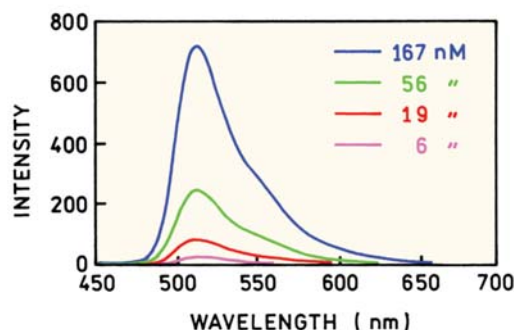
Figure 2.37. CCD spectrofluorometer and emission spectra of fluorescein. The light source for the fluorescein spectra was a 450 nm blue LED. From [25]. Image courtesy of Ocean Optics Inc.

ic range. CCDs typically contain 10^6 or more pixels. Each pixel acts as an accumulating detector where charge accumulates in proportion to total light exposure. The charge at each pixel point can be read out when desired, to obtain a two-dimensional image. CCDs are used widely in fluorescence microscopy.[23–24]

Small spectrofluorometers using CCDs are commercially available.[25] These devices are conveniently interfaced via a USB cable and have no moving parts. The sensitivity can be rather good, as seen from the fluorescein emission spectra (Figure 2.37). The signal is easily brought to the device using a fiber-optic cable. When combined with an LED light source the entire instrument becomes a solid-state device. These spectrofluorometers are convenient for bringing the instrument to the experiment, rather than vice versa.

2.7. POLARIZERS

When discussing polarizers it is useful to recall a few conventional definitions. The laboratory vertical-axis is typically referred to as the *z*-axis. Light can be described as
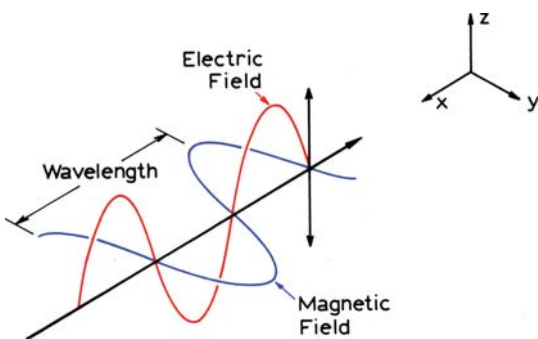
Figure 2.38. Vertically polarized light.

Figure 2.40. Transmission of light through polarizers. The incident beam is unpolarized. Only vertically polarized light passes through the first polarizer. Transmission through the second polarizer is proportional to $\cos^2 \theta$.

having a direction for its electrical component. Unpolarized light, of the type from incandescent or arc lamp sources, has equal amplitudes of the electric vector normal to the direction of light propagation. Polarized light has greater amplitude in one of the directions. Light with its electrical vector directed along the z-axis is said to be vertically polarized (Figure 2.38). Light with its electrical vector at right angles to the z-axis is said to be horizontally polarized.

In a discussion of polarization, the terms "S" and "P" polarization are often used. These terms are defined relative to the normal to the plane of incidence of the light on the optical interface. The plane of incidence is the plane defined by the light ray and the axis normal to the surface. If the electrical vector is in the plane of incidence the ray is said to be "P" polarized (Figure 2.39). If the electrical vector is perpendicular to the plane of incidence this ray is said to be "S" polarized.

Polarizers transmit light when the electric vector is aligned with the polarization axis, and block light when the

electric vector is rotated $90°$. These principles are shown in Figure 2.40. The incident light is unpolarized. About 50% of the light is transmitted by the first polarizer, and this beam is polarized along the principal axis of the polarizer. If the second polarizer is oriented in the same direction, then all the light is transmitted except for reflection losses. If the second polarizer is rotated through an angle θ the intensity is given by

$$I = I_{max} \cos^2 \theta \qquad (2.2)$$

where I_{max} corresponds to $\theta = 0$. Polarizers are frequently characterized by their extinction ratios. If the first polarizer is illuminated with linearly polarized light along the principal axis, the extinction ratio is the ratio of intensities for parallel ($\theta = 0°$) and crossed polarizers ($\theta = 90$). A slightly different definition is used if the first polarizer is illuminated with unpolarized light. Extinction ratios range from 10^3 to 10^6.

For general use in fluorescence spectroscopy a UV-transmitting Glan-Thompson polarizer has the best all-around properties (Figure 2.41). These polarizers consist of calcite prisms, which are birefringent, meaning the refractive index is different along each optical axis of the crystal. The angle of the crystal is cut so that one polarized component undergoes total internal reflection at the interface, and the other continues along its optical path. The reflected beam is absorbed by the black material surrounding the calcite. The purpose of the second prism is to ensure that the desired beam exits the polarizer in the same direction as the entering beam. For high-power laser applications an exit port is provided to allow the reflected beam to escape.
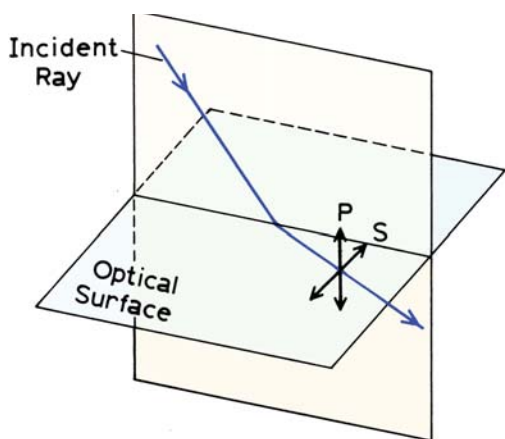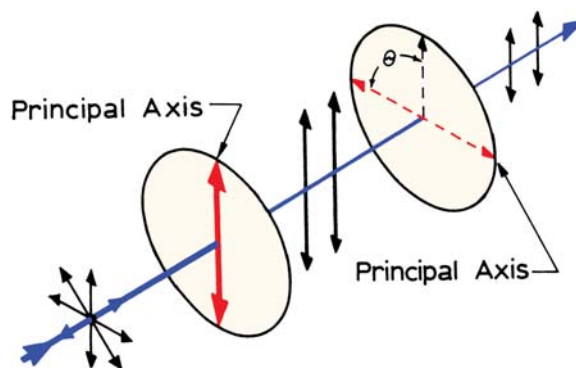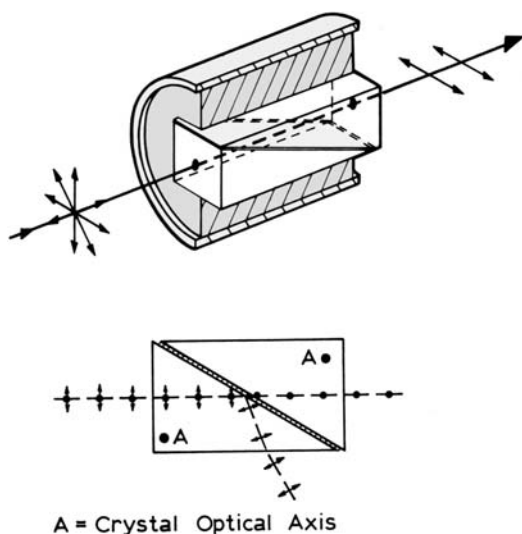

Figure 2.39. Definition of S and P polarization. P-polarized light has the electric field polarized parallel to the plane of incidence. S-polarized light has the electric field polarized perpendicular to the plane of incidence.

A = Crystal Optical Axis

Figure 2.41. Glan-Thompson polarizer (top) and light paths (bottom).

Calcite transmits well into the UV, and the transmission properties of the polarizer are determined by the material between the two prisms, which can be air or some type of cement. An air space is usually used for UV transmission. The polarizers are typically mounted in 1 inch diameter cylinders for ease of handling. Glan-Thompson polarizers provide high extinction coefficients near 10^6, but that is not the reason they are used in fluorescence. Glan-Thompson polarizers have a high acceptance angle, 10-15°, allowing them to be used where the beams are not well collimated. Another advantage is the low UV and visible absorbance of calcite, providing high transmission efficiency.

Another type of polarizer used in fluorescence are film polarizers, the same type used in polaroid glasses. These are thin films of a stretched polymer that transmit the light polarized in one direction and absorb the light polarized in another direction (Figure 2.40). Because the light is absorbed they are easily damaged by intense laser beams. They have a wide acceptance angle, but overall transmission is poor, especially in the ultraviolet. A wide variety of other polarizers are available. Most of the others, such as Wallaston polarizers and Rachon prism polarizers, split the unpolarized light into two beams, which must then be spatially selected.

2.8. CORRECTED EXCITATION SPECTRA

The development of methods to obtain excitation and emission spectra, corrected for wavelength-dependent effects, has been the subject of numerous investigations. None of these methods are completely satisfactory, especially if the corrected spectra are needed on a regular basis. Prior to correcting spectra, the researcher should determine if such corrections are necessary. Frequently, it is only necessary to compare emission spectra with other spectra collected on the same instrument. Such comparisons are usually made between the technical (or uncorrected) spectra. Furthermore, the response of many spectrofluorometers is similar because of the similar components, and comparison with spectra in the literature can frequently be made. Of course, the spectral distributions and emission maxima will differ slightly, but rigorous overlap of spectra obtained in different laboratories is rarely a necessity.

Modern instruments with red-sensitive PMTs and with gratings comparable to that shown in Figure 2.41 can provide spectra that are not very distorted, particularly in the visible to red region of the spectrum. Corrected spectra are needed for calculation of quantum yields and overlap integrals (Chapter 13). We briefly describe the methods judged to be most useful.

2.8.1. Corrected Excitation Spectra Using a Quantum Counter

Excitation spectra are distorted primarily by the wavelength dependence of the intensity of the exciting light. This intensity can be converted to a signal proportional to the number of incident photons by the use of a quantum counter. Rhodamine B (RhB) in ethylene glycol (3 g/l) is the best-known quantum counter,[26] and to this day remains the most generally reliable and convenient quantum counter. This concentrated solution absorbs virtually all incident light from 220 to 600 nm. The quantum yield and emission maximum ($\approx$630 nm) of rhodamine B are essentially independent of excitation wavelength from 220 to 600 nm.

The principle of a quantum counter is illustrated in Figure 2.42, which shows the ratio of the intensities observed from the RhB quantum counter and a thermopile. It is seen that the ratio remains constant at varying wavelengths. Since the emission spectrum of rhodamine B is independent of excitation wavelength, the quantum counter circumvents the wavelength-dependent sensitivity of the reference phototube. Hence, this solution provides a signal of constant emission wavelength and this signal, which is proportional to the photon flux of the exciting light. Quantum counters can also be made using moderately concentrated solutions of quinine sulfate or fluorescein. Quinine sulfate (4 g/l in 1
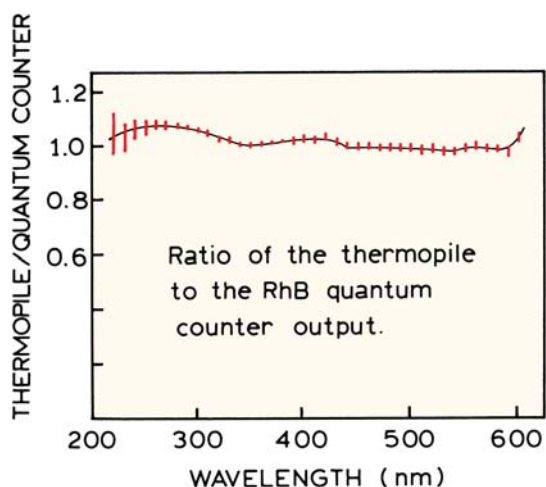
Figure 2.42. Comparison of the thermopile and the rhodamine B quantum counter as radiation detectors. Redrawn from [26].

Table 2.3. Quantum Counters

Solution	Range (nm)	Flatness	Reference
3 g/l Rhodamine B in ethylene glycol	220–580	±5%	26
8 g/l Rhodamine B in ethylene glycol[a]	250–600	±4%	27
2 g/l Fluorescein in 0.1 N NaOH	240–400[b]	±5%	26
4 g/l quinine sulfate in 1 N H_2SO_4	220–340	±5%	26
Rhodamine in polyvinyl alcohol (PVA) films	360–600	±3%	28[c]
Coumarins in PVA films	360–480	±3%	28[c]
5 g/l $Ru(bpy)_3^{2+}$ in methanol	360–540	1.1%	29
$Ru(bpy)_3^+$ in PVA films	360–530	1%	29[d]
8 g/l HITC[e] in acetonitrile	320–800[f]	±10%	30

[a]A higher concentration of RhB is claimed to be preferred for use in transmission mode. See [27].

[b]Response may be 15% lower from 340 to 360 nm.

[c]See [28] for details on the rhodamines, coumarins, and PVA film preparations.

[d]See [29] for details.

[e]HITC, 1,1',3,3,3',3'-hexamethylindotricarbocyanine.

[f]Deviation up to 20% occurs near 470 nm.

N H_2SO_4) is useful at excitation wavelengths ranging from 220 to 340 nm and fluorescein (2 g/l in 0.1 N NaOH) is useful over this same range, but is less reliable from 340 to 360 nm,[26] where absorption of fluorescein is weaker.

To record corrected excitation spectra, the quantum counter is placed in the reference channel of the spectrofluorometer (Figure 2.1). Because of the high optical density, the reference cell holder is modified so that the emission is observed from the same surface of the quantum counter that is being illuminated. Alternatively, quantum counters can be used in a transmission mode by observing the fluorescent light exiting the back surface of the illuminated cuvette.[27] In either case an optical filter is placed between the quantum counter and the PMT, which eliminates incident light but transmits the fluorescence. With a quantum counter in place, a corrected excitation spectrum may be obtained by scanning the excitation monochromator and measuring the ratio of the fluorescence intensity from the sample to that from the quantum counter. The wavelength-dependent response of the emission monochromator and phototube are not important because the emission wavelength is unchanged during a scan of the excitation wavelength. This procedure was used to record the corrected excitation spectrum of fluorescein shown in Figure 2.6.

Other quantum counters have been described, and are summarized in Table 2.3. The long wavelength dye HITC extends the range to 800 nm, but its response is not as flat as RhB. Unfortunately, there is no perfect quantum counter, and for most applications RhB appears to be the best choice.

2.9. CORRECTED EMISSION SPECTRA

2.9.1. Comparison with Known Emission Spectra

It is necessary to know the wavelength-dependent efficiency of the detection system to calculate the corrected emission spectra. It is difficult and time consuming to measure the correction factors for any given spectrofluorometer. Even after careful corrections are made the results are only accurate to ±10%. For this reason the observed technical spectra are usually reported. If corrected spectra are necessary, one simple and reliable method of obtaining the necessary correction factors is to compare the observed emission spectrum of a standard substance with the known corrected spectrum for this same substance. Such spectra have been published for a variety of readily available fluorophores including quinine sulfate, β-naphthol, 3-aminophthalimide, 4-dimethylamino-4'-nitrostilbene, and N,N-dimethylamino-m-nitrobenzene.[31–36] The emission wavelengths of these compounds cover the range from 300 to 800 nm and the data are presented in graphical and numerical form. Corrected spectra have been published for a series of harmine derivatives, covering the range 400–600

nm.[37] For convenience some of these corrected spectra are given in Appendix I, Corrected Emission Spectra.

To obtain correction factors the emission spectrum of a standard compound is recorded and compared to the data for a standard compound. This simple comparative method avoids the difficulties inherent in the more rigorous procedures described below. β-Naphthol should probably not be used as a standard because, under the conditions described, both naphthol and naphtholate emission are observed. The dual emission is a result of an excited state reaction, the extent of which is difficult to control. Quinine sulfate has been questioned as a standard, because its intensity decay may not be a single exponential and its quantum yield may be somewhat dependent on excitation wavelength.[38] However, it seems to be an acceptable standard for most circumstances. One should remember that quinine sulfate is collisionally quenched by chloride,[39] so solutions of quinine used as a quantum yield standard should not contain chloride. A potentially superior standard is β-carboline, whose spectral characteristics are similar to quinine sulfate and which displays a single exponential decay time.[40] The emission spectra of quinine sulfate and β-carboline are similar.

2.9.2. Corrections Using a Standard Lamp

The correction factors can also be obtained by observing the wavelength-dependent output from a calibrated light source. The wavelength distribution of the light from a tungsten filament lamp can be approximated by that of a black body of equivalent temperature. Standard lamps of known color temperature are available from the National Bureau of Standards and other secondary sources. Generally one uses the spectral output data provided with the lamp ($L(\lambda)$) because the black-body equation is not strictly valid for a tungsten lamp. The detection system is then calibrated as follows:

1. The intensity of the standard lamp versus wavelength $I(\lambda)$ is measured using the detection system of the spectrofluorometer.
2. The sensitivity of the detection system $S(\lambda)$ is calculated using

$$S(\lambda) = I(\lambda)/L(\lambda) \qquad (2.3)$$

   where $L(\lambda)$ is the known output of the lamp.
3. The corrected spectra are then obtained by dividing the measured spectra by these sensitivity factors.

It is important to recognize that the operation of a standard lamp requires precise control of the color temperature. In addition, the spectral output of the lamp can vary with age and usage of the lamp.

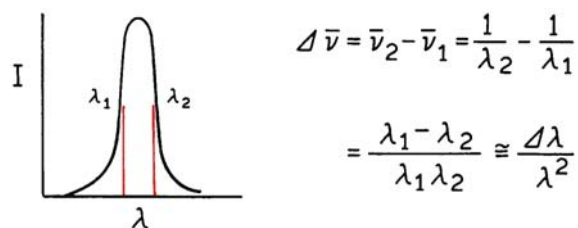## 2.9.3. Correction Factors Using a Quantum Counter and Scatterer

Another method to obtain the correction factors for the emission monochromator and PMT is to calibrate the xenon lamp in the spectrofluorometer for its spectral output.[26] The relative photon output ($L(\lambda)$) can be obtained by placing a quantum counter in the sample compartment. Once this intensity distribution is known, the xenon lamp output is directed onto the detector using a magnesium oxide scatterer. MgO is assumed to scatter all wavelengths with equal efficiency. Correction factors are obtained as follows:

1. The excitation wavelength is scanned with the quantum counter in the sample holder. The output yields the lamp output $L(\lambda)$.
2. The scatterer is placed in the sample compartment and the excitation and emission monochromators are scanned in unison. This procedure yields the product $L(\lambda)\,S(\lambda)$, where $S(\lambda)$ is the sensitivity of the detector system.
3. Division of $S(\lambda) \bullet L(\lambda)$ by $L(\lambda)$ yields the sensitivity factors $S(\lambda)$.

A critical aspect of this procedure is obtaining a reliable scatterer. The MgO must be freshly prepared and be free of impurities. Although this procedure seems simple, it is difficult to obtain reliable correction factors. It is known that the reflectivity of MgO changes over time, and with exposure to UV light, particularly below 400 nm.[41] In addition to changes in reflectivity, it seems probable that the angular distribution of the scattered light and/or collection efficiency changes with wavelength, and one should probably use an integrating sphere at the sample location to avoid spatial effects. Given the complications and difficulties of this procedure, the use of emission spectrum standards is the preferred method when corrected emission spectra are needed.

2.9.4. Conversion Between Wavelength and Wavenumber

Occasionally, it is preferable to present spectra on the wavenumber scale (γ) rather than on the wavelength scale

$$\Delta \bar{\nu} = \bar{\nu}_2 - \bar{\nu}_1 = \frac{1}{\lambda_2} - \frac{1}{\lambda_1}$$

$$= \frac{\lambda_1 - \lambda_2}{\lambda_1 \lambda_2} \cong \frac{\Delta \lambda}{\lambda^2}$$

Figure 2.43. Relationship between spectral resolution in wavelength (λ) or wavenumber ($\bar{\nu}$).

(λ). Wavelengths are easily converted to wavenumbers (cm^{-1}) simply by taking the reciprocal. However, the bandpass in wavenumbers is not constant when the spectrum is recorded with constant wavelength resolution, as is usual with grating monochromators. For example, consider a constant bandpass $\Delta \lambda = \lambda_2 - \lambda_1$, where λ_1 and λ_2 are wavelengths on either side of the transmission maximum (Figure 2.43). At 300 nm a bandpass ($\Delta \lambda$) of 2 nm is equivalent to 222 cm^{-1}. At 600 nm, this same bandpass is equivalent to a resolution (Δ) of 55 cm^{-1}. As the wavelength is increased, the bandpass (in cm^{-1}) decreases as the square of the exciting wavelength. From $\bar{\gamma} = 1/\lambda$, it follows that $|\Delta \nu| = |\Delta \lambda|/\lambda^2$. Therefore, if spectra are obtained in the usual form of intensity per wavelength interval $I(\lambda, \lambda + \Delta \lambda)/\Delta \lambda$ and $I(\bar{\nu}) = I(\bar{\nu}, \bar{\nu} + \Delta \bar{\nu})$, then conversion to the wavenumber scale requires[38–40] that each intensity be multiplied by λ^2:

$$I(\bar{\nu}) = \lambda^2 I(\lambda) \tag{2.4}$$

The effect of this wavelength-to-wavenumber conversion is illustrated in Appendix I. Multiplication by λ^2 results in selective enhancement of the long-wavelength side of the emission, and there is a shift in the apparent emission maximum. It should be noted that even after this correction is performed the resolution of the spectrum still varies with wavenumber.

2.10. QUANTUM YIELD STANDARDS

The easiest way to estimate the quantum yield of a fluorophore is by comparison with standards of known quantum yield. Some of the most used standards are listed in Table 2.4. The quantum yields of these compounds are mostly independent of excitation wavelength, so the standards can be used wherever they display useful absorption.

Determination of the quantum yield is generally accomplished by comparison of the wavelength integrated intensity of the unknown to that of the standard. The optical density is kept below 0.05 to avoid inner filter effects, or the optical densities of the sample and reference (r) are matched at the excitation wavelength. The quantum yield of the unknown is calculated using

$$Q = Q_R \frac{I}{I_R} \frac{OD_R}{OD} \frac{n^2}{n_R^2} \tag{2.5}$$

Table 2.4. Quantum Yield Standards

Compound	Solvent	λ_{ex} (nm)	°C	Q	Reference
Quinine sulfate	0.1 M H_2SO_4	350	22	0.577	45
		366	–	0.53 ± 0.023	46
β-Carboline[a]	1 N H_2SO_4	350	25	0.60	40
Fluorescein	0.1 M NaOH	496	22	0.95 ± 0.03	47
9,10-DPA[b]	cyclohexane	–	–	0.95	48
9,10-DPA	"	366	–	1.00 ± 0.05	49–50
POPOP[c]	cyclohexane	–	–	0.97	48
2-Aminopyridine	0.1 N H_2SO_4	285	–	0.60 ± 0.05	50–51
Tryptophan	water	280	–	0.13 ± 0.01	52
Tyrosine	water	275	23	0.14 ± 0.01	52
Phenylalanine	water	260	23	0.024	52
Phenol	water	275	23	0.14 ± 0.01	52
Rhodamine 6G	ethanol	488	–	0.94	53
Rhodamine 101	ethanol	450–465	25	1.0	54
Cresyl Violet	methanol	540–640	22	0.54	55

[a]β-carboline is 9H-pyrido[3,4-β]-indole.
[b]9,10-DPA, 9,10-diphenylanthracene.
[c]POPOP, 2,2'-(1,4-phenylene)bis[5-phenyloxazole].
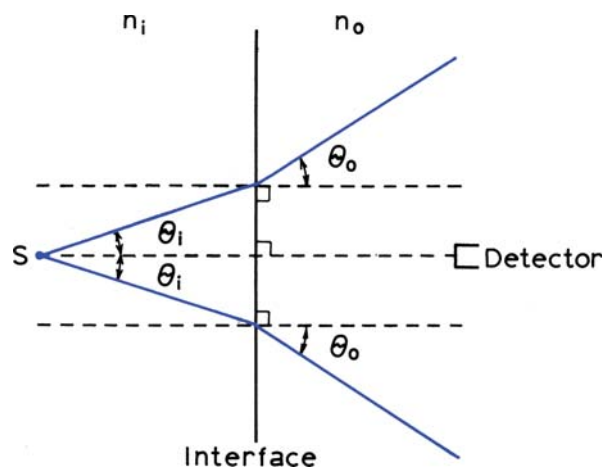
Figure 2.44. Refractive index effects in quantum yield measurements. The point source, S, is in a medium of refractive index n_i, the detector in a medium of refractive index n_0. $n_0 < n_i$. Reprinted with permission from [42], copyright © 1971, American Chemical Society.

where Q is the quantum yield, I is the integrated intensity, OD is the optical density, and n is the refractive index. The subscript R refers to the reference fluorophore of known quantum yield. In this expression it is assumed that the sample and reference are excited at the same wavelength, so that it is not necessary to correct for the different excitation intensities of different wavelengths.

This expression is mostly intuitive, except for the use of the ratio of refractive indices of the sample (n) and reference (n_R). This ratio has its origin in consideration of the intensity observed from a point source in a medium of refractive index n_i, by a detector in a medium of refractive index n_0 (Figure 2.44). The observed intensity is modified[42–43] by the ratio $(n_i/n_0)^2$. While the derivation was for a point source, the use of the ratio was found to be valid for many detector geometries.[44]

2.11. EFFECTS OF SAMPLE GEOMETRY

The apparent fluorescence intensity and spectral distribution can be dependent upon the optical density of the sample, and the precise geometry of sample illumination. The most common geometry used for fluorescence is right-angle observation of the center of a centrally illuminated cuvette (Figure 2.45, top left). Other geometric arrangements include front-face and off-center illumination. Off-center illumination decreases the path length, which can also be accomplished by using cuvettes with path lengths less than 1 cm. These methods are generally used to
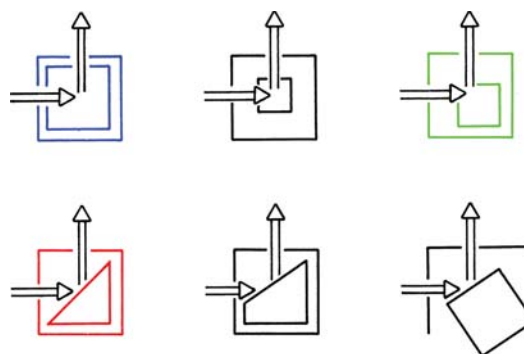

Figure 2.45. Various geometric arrangements for observation of fluorescence.

decrease the inner filtering effects due to high optical densities or to sample turbidity.

Frequently, front-face illumination is performed using either triangular cuvettes or square cuvettes oriented at 30 to 60° relative to the incident beam (Figure 2.45). In our opinion, an angle of 45° should be discouraged. A large amount of light is reflected directly into the emission monochromator, increasing the chance that stray light will interfere with the measurements. With front-face illumination we prefer to orient the illuminated surface about 30° from the incident beam. This procedure has two advantages. First, less reflected light enters the emission monochromator. Second, the incident light is distributed over a larger surface area, decreasing the sensitivity of the measurement to the precise placement of the cuvette within its holder. One disadvantage of this orientation is a decreased sensitivity because a larger fraction of the incident light is reflected off the surface of the cuvette.

It is important to recognize that fluorescence intensities are proportional to the concentration over only a limited range of optical densities. Consider a 1 x 1 cm cuvette that is illuminated centrally and observed at a right angle (Figure 2.45, top left). Assume further that the optical density at the excitation wavelength is 0.1. Using the definition of optical density ($\log I_0/I = OD$), the light intensity at the center of the cuvette (I) is $0.88I_0$, where I_0 is the intensity of the light incident to the cuvette. Since the observed fluorescence intensity is proportional to the intensity of the exciting light, the apparent quantum yield will be about 10% less than that observed for an infinitely dilute solution. This is called an inner filter effect. These effects may decrease the intensity of the excitation at the point of observation, or decrease the observed fluorescence by absorption of the fluorescence. The relative importance of each process depends
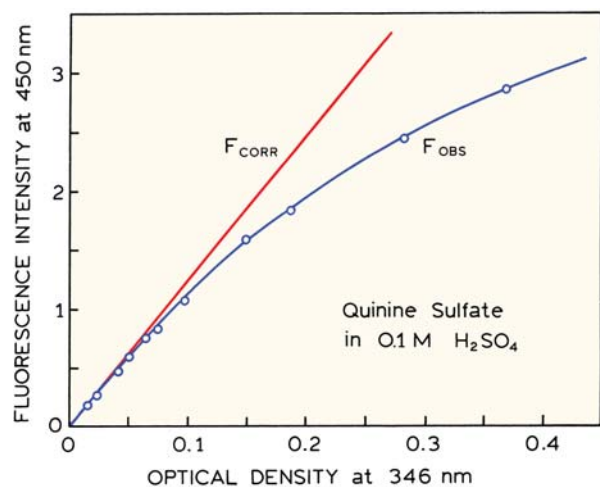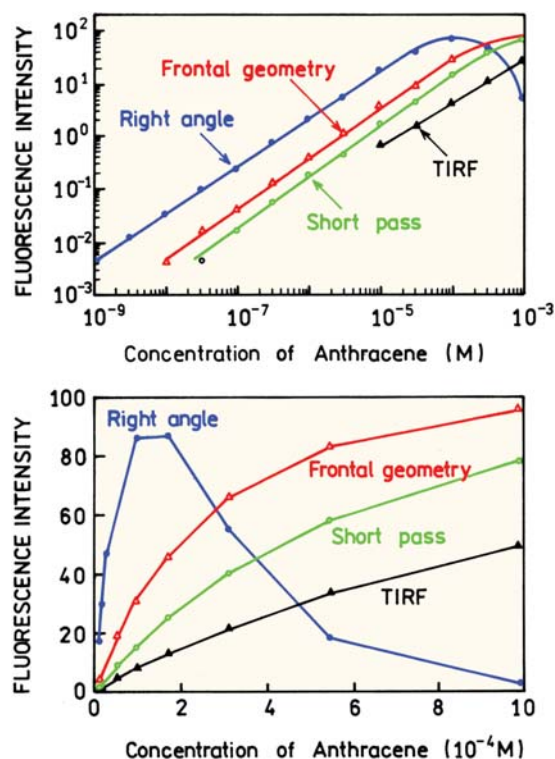
Figure 2.46. Effects of optical density on the fluorescence intensity of quinine sulfate. The solid line (——) shows the measured intensities, and the dashed line (– – –) indicates the corrected intensities, according to equation (2.6) with $OD_{em} = 0$. These data were obtained in a 1-cm^2 cuvette that was centrally illuminated.

Figure 2.47. Effect of concentrations on the intensity of anthracene. Short pass refers to a 1 mm x 10 mm cuvette. Revised from [61].

upon the optical densities of the sample at the excitation and emission wavelengths.

The data for quinine sulfate in Figure 2.46 illustrates the effect of optical density on fluorescence intensity. The measured intensity is proportional to optical density only to an optical density of 0.05. The linear range of the fluorescence intensities could be expanded by using off-center illumination, which reduces the effective light path. These intensities can be approximately corrected for the inner filter effects as follows. Suppose the sample has a significant optical density at both the excitation and emission wavelengths, OD_{ex} and OD_{em}, respectively. These optical densities attenuate the excitation and emission by $10^{-0.5OD_{ex}}$ and $10^{-0.5OD_{em}}$, respectively. Attenuation due to absorption of the incident light or absorption of the emitted light are sometimes called the primary and secondary inner filter effects, respectively.[56–57] The corrected fluorescence intensity is given approximately by

$$F_{corr} = F_{obs} \text{ antilog} \left(\frac{OD_{ex} + OD_{em}}{2} \right) \qquad (2.6)$$

The corrected intensities for quinine sulfate are shown in Figure 2.46, and these calculated values are seen to match the initial linear portion of the curve. For precise corrections it is preferable to prepare calibration curves using the precise compounds and conditions that will be used for the actual experimentation. Empirical corrections are typi-

cally used in most procedures to correct for sample absorbance.[56–60]

Figure 2.47 shows the effect of anthracene concentration on its emission intensity as observed for several geometries. TIRF refers to total internal reflection, which is described in Chapter 23. Short pass refers to a cuvette, 1 by 10 mm in dimension. The highest signal levels were obtained with the standard right-angle geometry. The linear range can be somewhat extended by using other geometries. Intuitively we may expect that with the front-face geometry the intensity will become independent of fluorophore concentration at high concentrations.[60,62] Under these conditions all the incident light is absorbed near the surface of the cuvette. Front-face illumination is also useful for studies of optically dense samples such as whole blood, or a highly scattering solution. The intensity is expected to be proportional to the ratio of the optical density of the fluorophore to that of the sample.[63] When front-face illumination is used the total optical density can be very large (20 or larger). However, high fluorophore concentrations can result in quenching due to a variety of interactions, such as radiative and non-radiative transfer and excimer formation. Fluo-
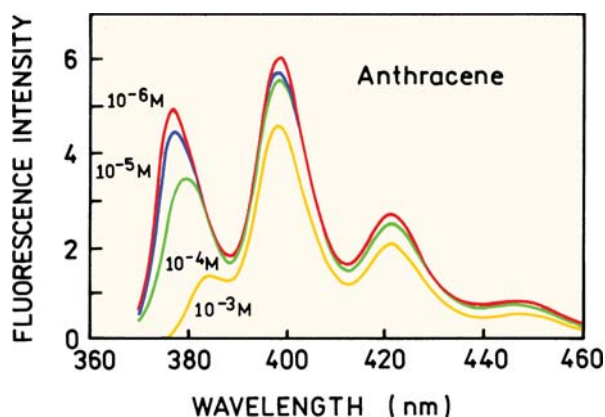
Figure 2.48. Effects of self-absorption of anthracene on its emission spectrum. A 1-cm^2 cuvette was used with right-angle observation. Revised from [61].

rophores like fluorescein with a small Stokes shift are particularly sensitive to concentration quenching.

High optical densities can distort the emission spectra as well as the apparent intensities. For example, when right-angle observation is used, the short-wavelength emission bands of anthracene are selectively attenuated (Figure 2.48). This occurs because these shorter wavelengths are absorbed by anthracene. Attenuation of the blue edge of the emission is most pronounced for fluorophores that have significant overlap of the absorption and emission spectra. Fluorophores that display a large Stokes shift are less sensitive to this phenomenon.

A dramatic effect of concentration can be seen with fluorophores that display a small Stokes shift. Figure 2.49 shows a photograph of three bottles of rhodamine 6G on a light box, with the concentration increasing from left to right. The color changes from green to orange. This effect is due to reabsorption of the shorter wavelength part of the emission. The emission spectra shift dramatically to longer wavelengths at higher concentrations.

2.12. COMMON ERRORS IN SAMPLE PREPARATION

It is valuable to summarize some of the difficulties that can be encountered with any given sample (Figure 2.50). The sample can be too concentrated, in which case all the light is absorbed at the surface facing the light source. In fact, this is one of the more common errors. With highly absorbing solutions and right-angle observations the signal levels can be very low. Other problems are when the sample contains a fluorescent impurity, or the detected light is contam-
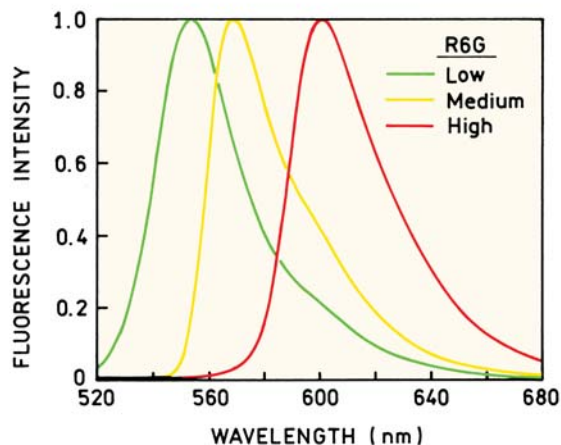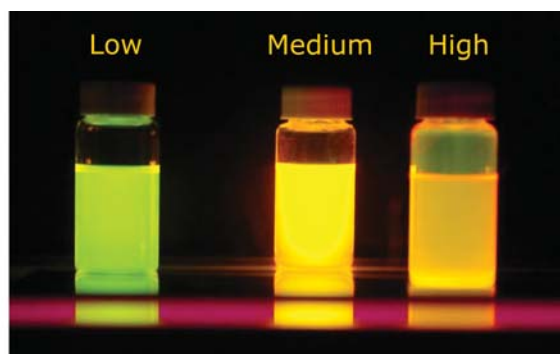
Figure 2.49. Effect of concentrations on the color and emission spectra of rhodamine 6G. The concentrations of R6G are 5 x 10^{-6}, 1.6 x 10^{-4}, and 5.7 x 10^{-3} M. From [64].

inated by Rayleigh or Raman scatter. Sometimes the signal may seem too noisy given the signal level. Intensity fluctuations can be due to particles that drift through the laser beam, and fluoresce or scatter the incident light.

Even if the fluorescence is strong, it is important to consider the possibility of two or more fluorophores, that is, an impure sample. Emission spectra are usually independent of excitation wavelength.[65] Hence it is useful to determine if the emission spectrum remains the same at different excitation wavelengths.
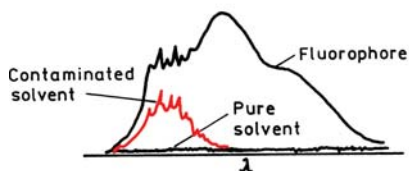
One example of a mixture of fluorophores is shown in Figure 2.51, which contains a mixture of coumarin 102 (C102) and coumarin 153 (C153). For a pure solution of C102 the same emission spectrum is observed for excitation at 360 and 420 nm (top). For a mixture of C102 and C153, one finds an increased intensity above 500 nm for excitation at 420 (bottom, dashed). This peak at 520 nm is due to C153, which can be seen from its emission spectrum (dot-
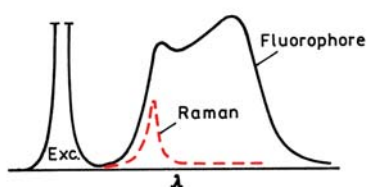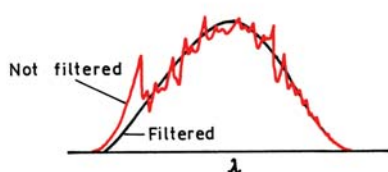
Figure 2.50. Common errors in sample preparation.

Figure 2.51. Emission spectra of C102 (top) and a mixture of C102 and C153 (bottom) excited at 360 and 420 nm. From [66].
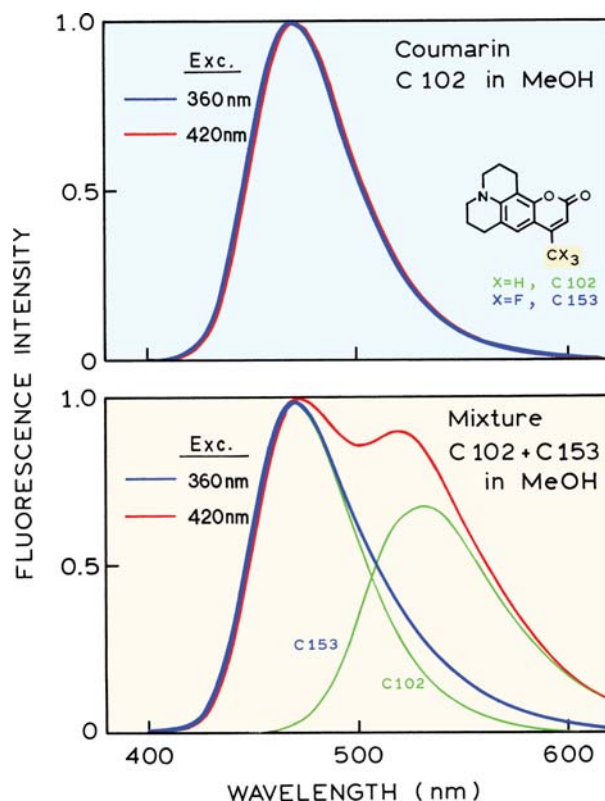
ted). Whenever the emission spectrum changes with excitation wavelength one should suspect an impurity.

It is interesting to note the significant change in the emission spectra of these two coumarin derivatives for a small change in structure. The fluorine-substituted coumarin (C153) appears to be more sensitive to solvent polarity. This effect is probably due to an increased charge separation in C153, due to movement of these amino electrons toward the $-CF_3$ group in the excited state. These effects are described in Chapter 6.

2.13. ABSORPTION OF LIGHT AND DEVIATION FROM THE BEER-LAMBERT LAW

A fundamental aspect of fluorescence spectroscopy is the measurement of light absorption. While the theory of light absorption is well known, a number of factors can result in misleading measurements of light absorption. We will first derive the Beer-Lambert Law, and then describe reasons for deviations from this law.

Consider a thin slab of solution of thickness dx that contains n light-absorbing molecules/cm^3 (Figure 2.52). Let σ be the effective cross-section for absorption in cm^2. The light intensity dI absorbed per thickness dx is proportional to the intensity of the incident light I and to both σ and n, where n is the number of molecules per cm^3:

$$\frac{dI}{dx} = -I\sigma n \tag{2.7}$$

Rearrangement and integration, subject to the boundary condition $I = I_0$ at $x = 0$, yields

$$\ln \frac{I_0}{I} = \sigma n d \tag{2.8}$$

where d is the thickness of the sample. This is the Beer-Lambert equation, which is generally used in an alternative form:
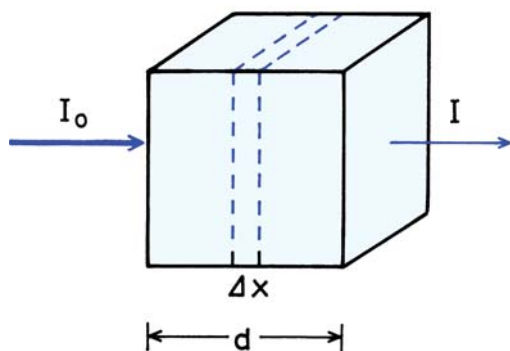
Figure 2.52. Light absorption.

$$\log \frac{I_0}{I} = \varepsilon c d = \text{optical density} \qquad (2.9)$$

where ε is the decadic molar extinction coefficient (in M^{-1} cm^{-1}) and c is the concentration in moles/liter. Combination of eqs. 2.8 and 2.9 yields the relationship between the extinction coefficient and the cross-section for light absorption:

$$\sigma = 2.303 \frac{\varepsilon c}{n} \qquad (2.10)$$

Since $n = Nc/10^3$ (where N is Avogadro's number), we obtain

$$\sigma = 3.82 \times 10^{-21} \varepsilon \quad (\text{in cm}^2) \qquad (2.11)$$

It is interesting to calculate the absorption cross-section for typical aromatic compounds. The extinction coefficients of anthracene are 160,000 and 6,300 M^{-1} cm^{-1} at 253 and 375 nm, respectively. These values correspond to cross-sections of 6.1 and 0.24 Å^2, respectively. Assuming the molecular cross-section of anthracene to be 12 Å^2, we see that anthracene absorbs about 50% of the photons it encounters at 253 nm and 2% of the photons at 375 nm.

Occasionally one encounters the term "oscillator strength." This term represents the strength of absorption relative to a completely allowed transition. The oscillator strength (f) is related to the integrated absorption of a transition by

$$f = \frac{4.39 \times 10^{-9}}{n} \int \varepsilon(\bar{\nu}) \, d\bar{\nu} \qquad (2.12)$$

where n is the refractive index.

2.13.1. Deviations from Beer's Law

Beer's Law predicts that the optical density is directly proportional to the concentration of the absorbing species. Deviations from Beer's law can result from both instrumental and intrinsic causes. Biological samples are frequently turbid because of macromolecules or other large aggregates that scatter light. The optical density resulting from scatter will be proportional to $1/\lambda^4$ (Rayleigh scattering), and may thus be easily recognized as a background absorption that increases rapidly with decreasing wavelength.

If the optical density of the sample is high, and if the absorbing species is fluorescent, the emitted light cannot reach the detector. This effect yields deviations from Beer's law that are concave toward the concentration axis. The fluorescence is omnidirectional, whereas the incident light is collimated along an axis. Hence, this effect can be minimized by keeping the detector distant from the sample, and thereby decreasing the efficiency with which the fluorescence emission is collected.

If the absorbing species is only partially soluble, it may aggregate in solutions at high concentrations. The absorption spectra of the aggregates may be distinct from the monomers. An example is the common dye bromophenol blue. At concentrations around 10 mg/ml it appears as a red solution, whereas at lower concentrations it appears blue. Depending upon the wavelength chosen for observation, the deviations from Beer's law may be positive or negative.

The factors described above were due to intrinsic properties of the sample. Instrumental artifacts can also yield optical densities that are nonlinear with concentration. This is particularly true at high optical densities. For example, consider a solution of indole with an optical density of 5 at 280 nm. In order to accurately measure this optical density, the spectrophotometer needs to accurately quantify the intensity of I_0 and I, the latter of which is 10^{-5} less intense than the incident light I_0. Generally, the stray light passed by the monochromator, at wavelengths where the compound does not absorb, are larger than this value. As a result, one cannot reliably measure such high optical densities unless considerable precautions are taken to minimize stray light.

2.14. CONCLUSIONS

At first glance it seems easy to perform fluorescence experiments. However, there are numerous factors that can compromise the data and invalidate the results. One needs to be constantly aware of the possibility of sample contamina-

tion, or contamination of the signal from scattered or stray light. Collection of emission spectra, and examination of blank samples, is essential for all experiments. One cannot reliably interpret intensity values, anisotropy, or lifetimes without careful examination of the emission spectra.

REFERENCES

1. Revised from commercial literature provided by SLM Instruments.
2. Revised from commercial literature provided by Molecular Devices, http://www.moleculardevices.com/pages/instruments/gemini.html.
3. Revised from commercial literature from Spectra Physics, www.spectra-physics.com.
4. Laczko G, Lakowicz JR, unpublished observations.
5. Oriel Corporation, 250 Long Beach Blvd., PO Box 872, Stratford, CT 06497: Light Sources, Monochromators and Spectrographs, Detectors and Detection Systems, Fiber Optics.
6. ILC Technology Inc. 399 West Joan Drive, Sunnyvale, CA 94089: Cermax Product Specifications for collimated and focused xenon lamps.
7. Ocean Optics product literature, http://www.oceanoptics.com/products/
8. Hart SJ, JiJi RD. 2002. Light emitting diode excitation emission matrix fluorescence spectroscopy. *Analyst* **127**:1643–1699.
9. Landgraf S. 2004. Use of ultrabright LEDs for the determination of static and time-resolved fluorescence information of liquid and solid crude oil samples. *J Biochem Biophys Methods* **61**:125–134.
10. Gryczynski I, Lakowicz JR, unpublished observations.
11. Optometrics USA Inc., Nemco Way, Stony Brook Industrial Park, Ayer, MA 01432: 1996 Catalog Optical Components and Instruments.
12. Castellano P, Lakowicz JR, unpublished observations.
13. Melles Griot product literature, http://shop.mellesgriot.com/products/optics/
14. Macleod HA. 2001. *Thin-film optical filters*, 3rd ed. Institute of Physics, Philadelphia.
15. Semrock Inc., Rochester, NY, www.semrock.com.
16. Gryczynski I, Malak H, Lakowicz JR, Cheung HC, Robinson J, Umeda PK. 1996. Fluorescence spectral properties of troponin C mutant F22W with one-, two- and three-photon excitation. *Biophys J* **71**:3448–3453.
17. Szmacinski H, Gryczynski I, Lakowicz JR. 1993. Calcium-dependent fluorescence lifetimes of Indo-1 for one- and two-photon excitation of fluorescence. *Photochem Photobiol* **58**:341–345.
18. Hamamatsu Photonics K.K., Electron Tube Center, (1994), 314-5, Shimokanzo, Toyooka-village, Iwata-gun, Shizuoka-ken, 438-01 Japan: Photomultiplier Tubes.
19. Provided by Dr. R. B. Thompson
20. Leaback DH. 1997. Extended theory, and improved practice for the quantitative measurement of fluorescence. *J Fluoresc* **7**(1):55S–57S.
21. Epperson PM, Denton MB. 1989. Binding spectral images in a charge-coupled device. *Anal Chem* **61**:1513–1519.
22. Bilhorn RB, Sweedler JV, Epperson PM, Denton MB. 1987. Charge-transfer device detectors for analytical optical spectroscopy—operation and characteristics. *Appl Spectrosc* **41**:1114–1124.
23. Hiraoka Y, Sedat JW, Agard DA. 1987. The use of a charge-coupled device for quantitative optical microscopy of biological structures. *Science* **238**:36–41.
24. Aikens RS, Agard DA, Sedat JW. 1989. Solid-state imagers for microscopy. *Methods Cell Biol* **29**:291–313.
25. Ocean Optics Inc., http://www.oceanoptics.com/products/usb2000 flg.asp.
26. Melhuish WH. 1962. Calibration of spectrofluorometers for measuring corrected emission spectra. *J Opt Soc Am* **52**:1256–1258.
27. Yguerabide J. 1968. Fast and accurate method for measuring photon flux in the range 2500-6000 Å. *Rev Sci Instrum* **39**(7):1048–1052.
28. Mandal K, Pearson TDL, Demas JN. 1980. Luminescent quantum counters based on organic dyes in polymer matrices. *Anal Chem* **52**:2184–2189.
29. Mandal K, Pearson TDL, Demas NJ. 1981. New luminescent quantum counter systems based on a transition-metal complex. *Inorg Chem* **20**:786–789.
30. Nothnagel EA. 1987. Quantum counter for correcting fluorescence excitation spectra at 320- and 800-nm wavelengths. *Anal Biochem* **163**:224–237.
31. Lippert E, Nagelle W, Siebold-Blakenstein I, Staiger U, Voss W. 1959. Messung von fluorescenzspektren mit hilfe von spektralphotometern und vergleichsstandards. *Zeitschr Anal Chem* **17**:1–18.
32. Schmillen A, Legler R. 1967. *Landolt-Borstein*. Vol 3: Lumineszenz Organischer Substanzen. Springer-Verlag, New York.
33. Argauer RJ, White CE. 1964. Fluorescent compounds for calibration of excitation and emission units of spectrofluorometer. *Anal Chem* **36**:368–371.
34. Melhuish WH. 1960. A standard fluorescence spectrum for calibrating spectrofluorometers. *J Phys Chem* **64**:762–764.
35. Parker CA. 1962. Spectrofluorometer calibration in the ultraviolet region. *Anal Chem* **34**:502–505.
36. Velapoldi RA. 1973. Considerations on organic compounds in solution and inorganic ions in glasses as fluorescent standard reference materials. *Proc Natl Bur Stand* **378**:231–244.
37. Pardo A, Reyman D, Poyato JML, Medina F. 1992. Some β-carboline derivatives as fluorescence standards. *J Lumines* **51**:269–274.
38. Chen RF. 1967. Some characteristics of the fluorescence of quinine. *Anal Biochem* **19**:374–387.
39. Verity B, Bigger SW. 1996. The dependence of quinine fluorescence quenching on ionic strength. *Int J Chem Kinet* **28**(12):919–923.
40. Ghiggino KP, Skilton PF, Thistlethwaite PJ. 1985. β-Carboline as a fluorescence standard. *J Photochem* **31**:113–121.
41. Middleton WEK, Sanders CL. 1951. The absolute spectral diffuse reflectance of magnesium oxide. *J Opt Soc Am* **41**(6):419–424.
42. Demas JN, Crosby GA. 1971. The measurement of photoluminescence quantum yields: a review. *J Phys Chem* **75**(8):991–1025.
43. Birks JB. 1970. *Photophysics of aromatic molecules*. Wiley-Interscience, New York.
44. Hermans JJ, Levinson S. 1951. Some geometrical factors in light-scattering apparatus. *J Opt Soc Am* **41**(7):460–465.
45. Eastman JW. 1967. Quantitative spectrofluorimetry—the fluorescence quantum yield of quinine sulfate. *Photochem Photobiol* **6**:55–72.
46. Adams MJ, Highfield JG, Kirkbright GF. 1977. Determination of absolute fluorescence quantum efficiency of quinine bisulfate in aqueous medium by optoacoustic spectrometry. *Anal Chem* **49**:1850–1852.
47. Brannon JH, Magde D. 1978. Absolute quantum yield determination by thermal blooming: fluorescein. *J Phys Chem* **82**(6):705–709.
48. Mardelli M, Olmsted J. 1977. Calorimetric determination of the 9,10-diphenyl-anthracene fluorescence quantum yield. *J Photochem* **7**:277–285.
49. Ware WR, Rothman W. 1976. Relative fluorescence quantum yields using an integrating sphere: the quantum yield of 9,10-diphenylanthracene in cyclohexane. *Chem Phys Lett* **39**(3):449–453.
50. Testa AC. 1969. Fluorescence quantum yields and standards. *Fluoresc News* **4**(4):1–3.

51. Rusakowicz R, Testa AC. 1968. 2-aminopyridine as a standard for low-wavelength spectrofluorometry. *J Phys Chem* **72**:2680–2681.
52. Chen RF. 1967. Fluorescence quantum yields of tryptophan and tyrosine. *Anal Lett* **1**:35–42.
53. Fischer M, Georges J. 1996. Fluorescence quantum yield of rhodamine 6G in ethanol as a function of concentration using thermal lens spectrometry. *Chem Phys Lett* **260**:115–118.
54. Karstens T, Kobe K. 1980. Rhodamine B and Rhodamine 101 as reference substances for fluorescence quantum yield measurements. *J Phys Chem* **84**:1871–1872.
55. Magde D, Brannon JH, Cremers TL, Olmsted J. 1979. Absolute luminescence yield of cresyl violet: a standard for the red. *J Phys Chem* **83**(6):696–699.
56. Kubista M, Sjöback R, Eriksson S, Albinsson B. 1994. Experimental correction for the inner-filter effect in fluorescence spectra. *Analyst* **119**:417–419.
57. Yappert MC, Ingle JD. 1989. Correction of polychromatic luminescence signals for inner-filter effects. *Appl Spectros* **43**(5):759–767.
58. Wiechelman KJ. 1986. Empirical correction equation for the fluorescence inner filter effect. *Am Lab* **18**:49–53.
59. Puchalski MM, Morra MJ, von Wandruszka R. 1991. Assessment of inner filter effect corrections in fluorimetry. *Fresenius J Anal Chem* **340**:341–344.
60. Guilbault GG, ed. 1990. *Practical fluorescence*. Marcel Dekker, New York.
61. Kao S, Asanov AN, Oldham PB. 1998. A comparison of fluorescence inner-filter effects for different cell configurations. *Instrum Sci Tech* **26**(4):375–387.
62. Eisinger J. 1969. A variable temperature, UV luminescence spectrograph for small samples. *Photochem Photobiol* **9**:247–258.
63. Eisinger J, Flores J. 1979. Front-face fluorometry of liquid samples. *Anal Biochem* **94**:15–21.
64. Courtesy of Drs. Joanna Lukomska and Ignacy Gryczynski.
65. Kasha M. 1960. Paths of molecular excitation. *Radiat Res* **2**:243–275.
66. Gryczynski I, unpublished observations.

PROBLEMS

P2.1. *Measurement of High Optical Densities*: Suppose you wish to determine the concentration of a 10^{-4} M solution of rhodamine B, which has an extinction coefficient near 100,000 M^{-1} cm^{-1} at 590 nm. The monochromator in your spectrophotometer is imperfect, and the incident light at 590 nm contains 0.01% of light at longer wavelengths, not absorbed by rhodamine B. What is the true optical density of the solution? Which is the apparent optical density measured with your spectrophotometer? Assume the path length is 1 cm.

P2.2. *Calculation of Concentrations by Absorbance*: Suppose a molecule displays an extinction coefficient of 30,000 M^{-1} cm^{-1}, and that you wish to determine its concentration from the absorbance. You have two solutions, with actual optical densities of 0.3 and 0.003 in a 1-cm cuvette. What are the concentrations of the two solutions? Assume the measurement error in percent transmission is 1%. How does the 1% error affect determination of the concentrations?